iScience

CellPress
OPEN ACCESS

Article

Intestinal microbial circadian rhythms drive sex differences in host immunity and metabolism

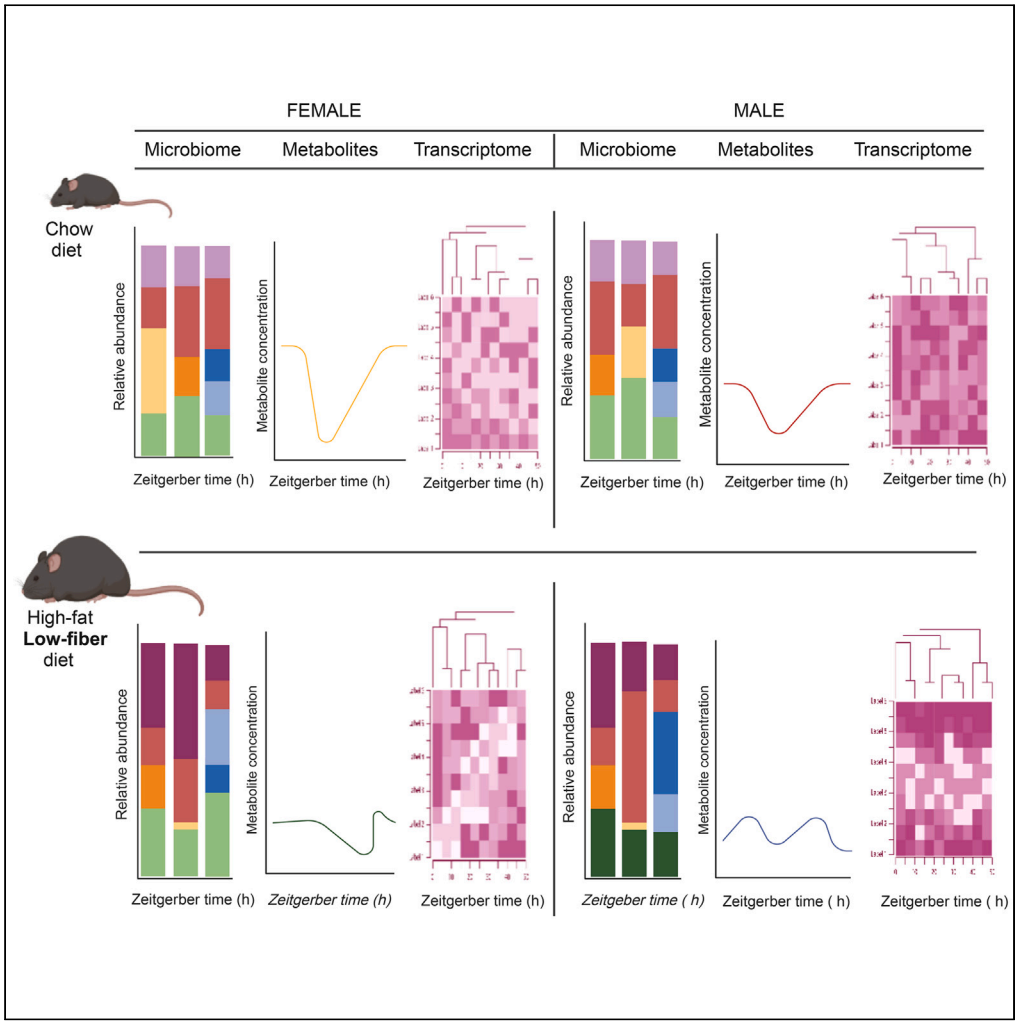

Sarah K. Munyoki, Julie P. Goff, Antonija Kolobaric, ..., Colleen A. McClung, Kathleen E. Morrison, Eldin Jašarević

eldin.jasarevic@pitt.edu

Highlights

Intestinal microbial circadian rhythms differ by sex

Sex-specific rhythms in host transcriptional networks are microbiome-dependent

Diet-induced obesity entrains new sex-specific microbial and host gene circadian rhythms

Timing of data collection influences the magnitude of sex differences

Munyoki et al., iScience 26, 107999
October 20, 2023
https://doi.org/10.1016/j.isci.2023.107999

iScience

CellPress
OPEN ACCESS

Article

Intestinal microbial circadian rhythms drive sex differences in host immunity and metabolism

Sarah K. Munyoki,[1,2,3] Julie P. Goff,[1,2,3] Antonija Kolobaric,[4] Armari Long,[1,2,3] Steven J. Mullett,[5,6] Jennifer K. Burns,[7,8] Aaron K. Jenkins,[7,8] Lauren DePoy,[7,8] Stacy G. Wendell,[5,6] Colleen A. McClung,[4,7,8] Kathleen E. Morrison,[9] and Eldin Jašarević[1,2,3,10,*]

SUMMARY

Circadian rhythms dynamically regulate sex differences in metabolism and immunity, and circadian disruption increases the risk of metabolic disorders. We investigated the role of sex-specific intestinal microbial circadian rhythms in host metabolism using germ-free and conventionalized mice and manipulation of dietary-derived fat, fiber, and microbiota-accessible carbohydrates. Our findings demonstrate that sex differences in circadian rhythms of genes involved in immunity and metabolism depend on oscillations in microbiota, microbial metabolic functions, and microbial metabolites. Further, we show that consuming an obesogenic, high-fat, low-fiber diet produced sex-specific changes in circadian rhythms in microbiota, metabolites, and host gene expression, which were linked to sex differences in the severity of metabolic dysfunction. Our results reveal that microbial circadian rhythms contribute to sex differences in immunity and metabolism and that dietary factors can entrain new circadian rhythms and modify the magnitude of sex differences in host-microbe circadian dynamics.

INTRODUCTION

Sex differences in physiologic, metabolic, immune, and behavioral processes are well-documented across all vertebrate species, including humans.[1–7] The maintenance of these sex differences depends on a complex interplay between genetic, environmental, and developmental factors.[1,2] One consequence of these biological sex differences is that most adult-onset diseases exhibit a sex-specific bias in prevalence, age of onset, severity, and treatment outcome.[6] For instance, autoimmunity, obesity, metabolic syndrome, and type 2 diabetes exhibit significant sex differences in disease management and treatment response to dietary and pharmacological interventions. Despite the clear links between sex-specific physiology and disease trajectories, the historical underrepresentation of women in these studies has created a barrier to uncovering underlying mechanisms that may provide novel insights into disease prevention, intervention, and treatment.

Microbial communities within the intestinal tract are critical in balancing metabolic homeostasis and dysfunction.[8,9] At birth, the microbial composition is similar between female and male mice until around puberty, when these communities begin to diverge until they reach steady-state sex differences in adulthood.[10] Although the adult intestinal microbiota is typically stable, recent studies suggest that the relative abundance of microbiota varies significantly throughout the day, coordinating with the circadian clock and feeding patterns to generate diurnal rhythms in energy homeostasis, lipid metabolism, innate immune function, and energy substrate provision to distal tissues.[11–15] Moreover, individual variability in environmental and lifestyle exposures, including jet lag, shift work, antibiotic exposure, altered feeding times, and consumption of highly processed diets, are associated with disruption to diurnal rhythms in gut microbiota.[16–21] This microbial circadian misalignment increases the risk for obesity, poor glycemic control, metabolic dysfunction, inflammation, and heightened susceptibility to disease.[22–26]

Peripheral circadian rhythms also influence the composition of microbial communities in a sex-specific manner. Deletion of *Bmal1*, the principal driver of the mammalian molecular clock, abolishes sex differences in the microbiota composition.[27] Furthermore, sex differences in hepatic gene expression, metabolism, and reproductive development are disrupted in germ-free mice, suggesting that microbial-derived signals are necessary for sex-specific development and phenotypes.[28]

[1]Department of Obstetrics, Gynecology and Reproductive Sciences, University of Pittsburgh School of Medicine, Pittsburgh, PA, USA
[2]Department of Computational and Systems Biology, University of Pittsburgh School of Medicine, Pittsburgh, PA, USA
[3]Magee-Womens Research Institute, Pittsburgh, PA, USA
[4]Center for Neuroscience, University of Pittsburgh, Pittsburgh, PA, USA
[5]Department of Pharmacology & Chemical Biology, University of Pittsburgh School of Medicine, Pittsburgh, PA, USA
[6]Health Sciences Mass Spectrometry Core, University of Pittsburgh School of Medicine, Pittsburgh, PA, USA
[7]Clinical Translational Science Institute, University of Pittsburgh School of Medicine, Pittsburgh, PA, USA
[8]Department of Psychiatry, University of Pittsburgh School of Medicine, Pittsburgh, PA, USA
[9]Department of Psychology, West Virginia University, Morgantown, WV, USA
[10]Lead contact
*Correspondence: eldin.jasarevic@pitt.edu
https://doi.org/10.1016/j.isci.2023.107999

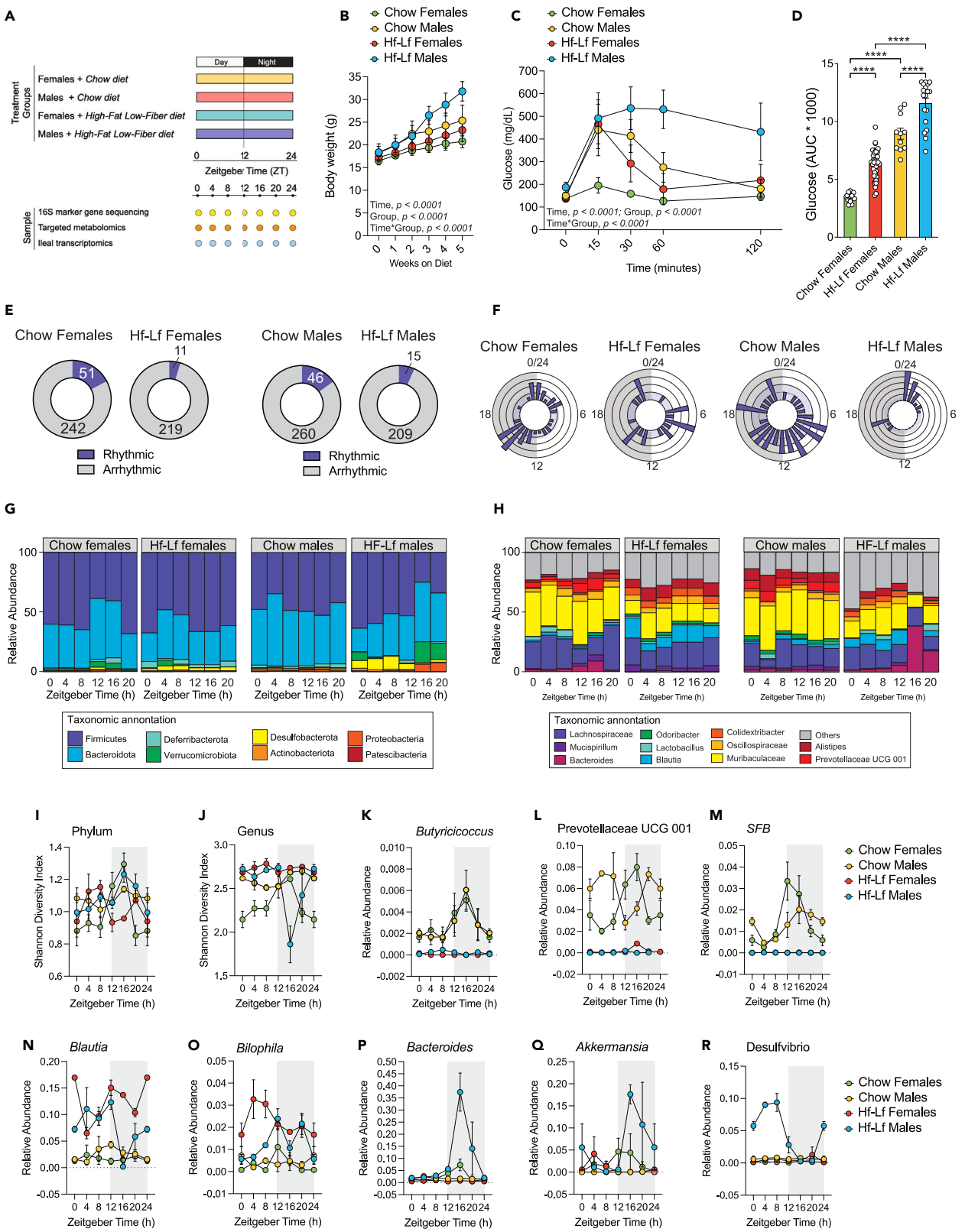
A
Treatment Groups
Females + Chow diet
Males + Chow diet
Females + High-Fat Low-Fiber diet
Males + High-Fat Low-Fiber diet
Day
Night
0 12 24
Zeitgeber Time (ZT)
0 4 8 12 16 20 24
Sample
16S marker gene sequencing
Targeted metabolomics
Ileal transcriptomics
B
Chow Females
Chow Males
Hf-Lf Females
Hf-Lf Males
Body weight (g)
Time, p < 0.0001
Group, p < 0.0001
Time*Group, p < 0.0001
Weeks on Diet
C
Chow Females
Chow Males
Hf-Lf Females
Hf-Lf Males
Glucose (mg/dL)
Time, p < 0.0001; Group, p < 0.0001
Time*Group, p < 0.0001
Time (minutes)
D
Glucose (AUC * 1000)
****
Chow Females
Hf-Lf Females
Chow Males
Hf-Lf Males
E
Chow Females
Hf-Lf Females
Chow Males
Hf-Lf Males
51
242
11
219
46
260
15
209
Rhythmic
Arrhythmic
F
Chow Females
Hf-Lf Females
Chow Males
Hf-Lf Males
0/24
6
12
18
G
Chow females
Hf-Lf females
Chow males
HF-Lf males
Relative Abundance
Zeitgeber Time (h)
Taxonomic annontation
Firmicutes
Bacteroidota
Deferribacterota
Verrucomicrobiota
Desulfobacterota
Actinobacteriota
Proteobacteria
Patescibacteria
H
Chow females
Hf-Lf females
Chow males
HF-Lf males
Relative Abundance
Zeitgeber Time (h)
Taxonomic annontation
Lachnospiraceae
Mucispirillum
Bacteroides
Odoribacter
Lactobacillus
Blautia
Colidextribacter
Oscillospiraceae
Muribaculaceae
Others
Alistipes
Prevotellaceae UCG 001
I
Phylum
Shannon Diversity Index
Zeitgeber Time (h)
J
Genus
Shannon Diversity Index
Zeitgeber Time (h)
K
Butyricicoccus
Relative Abundance
Zeitgeber Time (h)
L
Prevotellaceae UCG 001
Relative Abundance
Zeitgeber Time (h)
M
SFB
Relative Abundance
Zeitgeber Time (h)
Chow Females
Chow Males
Hf-Lf Females
Hf-Lf Males
N
Blautia
Relative Abundance
Zeitgeber Time (h)
O
Bilophila
Relative Abundance
Zeitgeber Time (h)
P
Bacteroides
Relative Abundance
Zeitgeber Time (h)
Q
Akkermansia
Relative Abundance
Zeitgeber Time (h)
R
Desulfvibrio
Relative Abundance
Zeitgeber Time (h)
Chow Females
Chow Males
Hf-Lf Females
Hf-Lf Males

Figure 1. Diet modifies sex differences in diurnal rhythmicity of the intestinal microbiota

(A) Schematic representation of study design and sample collections.

(B) Sex-specific effects of Chow and Hf-Lf diet on body weight gain (time*sex interaction, $F_{15, 419} = 38.75$, $p < 0.0001$). (a) Hf-Lf females weigh significantly more than Chow females ($t_{84} = 5.37$, $p = 0.0016$); (b) Hf-Lf males weigh significantly more than Chow males ($t_{84} = 4.041$, $p = 0.027$). (c) Chow males weigh significantly more than Hf-Lf females ($t_{84} = 4.973$, $p = 0.004$), showing that Hf-Lf female mice weigh less than Chow males even after 6weeks on Hf-Lf feeding.

(C) Sex-specific effects of Chow and Hf-Lf diet in glucose tolerance (time*sex interaction, $F_{12,316} = 33.82$, $p < 0.0001$). (a) Hf-Lf females showed significantly slower glucose clearance than Chow females ($t_{79} = 10.15$, $p < 0.0001$) and (b) Hf-Lf males showed significantly slower glucose clearance than Chow males ($t_{84} = 4.973$, $p = 0.004$). (c) Chow males showed similar glucose clearance as Hf-Lf females ($t_{79} = 2.803$, $p = 0.20$).

(D) Sex-specific effects of Chow and Hf-Lf diet on AUC of circulating glucose levels (main effect of treatment, $F_{3,79} = 107.7$, $p < 0.0001$). Hf-Lf females had higher glucose levels than Chow females ($t_{79} = 9.73$, $p < 0.0001$) and Hf-Lf males had higher glucose levels than Chow males ($t_{79} = 7.005$, $p < 0.0001$). Chow males had higher glucose levels than Hf-Lf females ($t_{79} = 7.835$, $p < 0.0001$).

(E) Sex differences in non-rhythmic and rhythmic microbiota detected in the cecum using cosinor analysis (Cosinor $p < 0.05$).

(F) Rose plot showing sex differences in acrophase distribution of microbiota in the cecum of adult females (left) and males (right).

(G) Relative abundance of top eight phyla across 24 h in Chow and Hf-Lf mice.

(H) Relative abundance of top twelve genera across 24 h in Chow and Hf-Lf mice.

(I) Phylum-level alpha diversity differed by time of day in males and females.

(J) Genus-level alpha diversity differed by time of day in males and females.

(K) Diurnal variation in *Butyricicoccus* relative abundance detected in Chow mice but lost in Hf-Lf mice.

(L) Diurnal variation in *Prevotellaceae UCG 001* relative abundance detected in Chow mice but lost in Hf-Lf mice.

(M) Diurnal variation in Segmented Filamentous Bacteria relative abundance detected in Chow mice but lost in Hf-Lf mice.

(N) Emergence of diurnal variation in *Blautia* relative abundance detected in Hf-Lf females relative to Hf-Lf males and Chow mice.

(O) Emergence of diurnal variation in *Bilophila* relative abundance detected in Hf-Lf females relative to Hf-Lf males and Chow mice.

(P) Emergence of diurnal variation in *Bacteroides* relative abundance detected in Hf-Lf males relative to Hf-Lf females and Chow mice.

(Q) Emergence of diurnal variation in *Akkermansia* relative abundance detected in Hf-Lf males relative to Hf-Lf females and Chow mice.

(R) Emergence of diurnal variation in *Desulfovibrio* relative abundance detected in Hf-Lf males relative to Hf-Lf females and Chow mice. Three murine-pathogen-free C57Bl/6NTac females and males were used for each condition, totaling 36 females and 36 males. Acrophases were calculated by cosinor analysis (period = 24 h). The threshold for the cosinor test was set to $p < 0.05$. Full cosinor analysis in Table S1. RM or One-way ANOVA, followed by Tukey correction for multiple testing. Data is represented as mean ± SEM. *$p < 0.05$, **$p < 0.01$, ***$p < 0.001$.

Dietary composition impacts rodents' circadian rhythms, from gene expression profiles to behavioral rhythms. Female and male mice exhibit stark differences when exposed to a high-fat diet.[29] Male mice display faster weight gain, increased pancreatic B-cell expansion, worsened glucose tolerance, and reduced insulin sensitivity compared to female mice on a high-fat diet.[29] High-fat diets have particularly damaging effects on circadian systems by blunting feeding behaviors.[30,31] High-fat diet-induced perturbations to the murine gut microbiome disrupt intestinal microbial circadian rhythms, altering host metabolic homeostasis leading to obesity and metabolic syndrome.[18,20,29] However, these studies were all conducted exclusively in male mice as the inclusion of females in obesity, microbiome, and circadian rhythms research has not been a common practice, resulting in a paucity of data regarding the effects of sex.[32]

This study aimed to identify sex-specific circadian rhythms in the murine gut microbial, metabolic, and transcriptional capacity under *ad libitium* feeding conditions. We used germ-free, conventionalized, and murine-pathogen-free mice and dietary manipulations to examine the central hypothesis that circadian rhythms in host-diet-microbe interactions differ between female and male mice. Despite the well-established observation that females are resistant to diet-induced obesity,[33,34] female mice are currently excluded in studies on circadian rhythms, diet-induced obesity, and the microbiome. To address this fundamental gap, we investigated whether circadian disruption caused by the consumption of a high-fat, low-fiber diet affects the microbiome, microbial metabolites, and host transcriptome in a sex-specific manner. To examine these hypotheses, we employed an integrated multi-Omics approach to identify sex differences in diurnal dynamics of the intestinal microbiota, microbial-derived metabolite production, systemic availability of microbial metabolites, and the host transcriptome.

RESULTS

Dietary factors link sex-specific circadian rhythms in gut microbiota composition to the severity of metabolic dysfunction

Host circadian rhythms, dietary inputs, and feeding behavior entrain the gut microbiome, influencing the timing and coordination of host metabolic processes.[19] High-fat diet disrupts circadian rhythms and alters the composition of the gut microbiota.[18] This disruption underlies many metabolic and inflammation-related disease processes.[35–37] Consumption of a high-fat, low-fiber (Hf-Lf) diet produces hallmark phenotypes of diet-induced obesity and metabolic syndrome, including increased rapid weight gain, excess accumulation of fat mass, hyperglycemia, hyperinsulinemia, metabolic endotoxemia, and low-grade chronic inflammation.[38–41] A more severe diet-induced metabolic phenotype is observed in male mice, while protection or resistance to diet-induced obesity is observed in female mice.[29,42] Hf-Lf feeding alters gut microbiota circadian rhythms in male mice, but the role of Hf-Lf induced obesity on female-specific microbial rhythms is unknown.[17,18,20] Although circadian disruption is often associated with sex-specific health outcomes, most studies on circadian rhythms, diet, the gut microbiome, and health outcomes often exclude female mice altogether. To investigate possible sex differences, we randomly assigned pubertal female and male mice to either a Hf-Lf diet (20% protein, 20% carbohydrate, 60% fat) or a chow diet (23.2% protein, 55.2% carbohydrate, 21.6% fat)[43,44] (Figure 1A). It is important to note that the lack of complex carbohydrates and soluble fibers in commercially available refined high-fat diet formulations (e.g., Research Diets OpenSource Diets) is proposed to be a contributing factor to excessive

weight gain, obesity and diabetes in mouse models of diet-induced metabolic syndrome and obesity. Hence, the dietary designation Hf-Lf highlights the absence of microbiota-accessible carbohydrates in these dietary formulations.[44–49]

To confirm diet-induced metabolic syndrome, mice were given *ad libitum* access to their respective diets throughout the experiment, and weekly body weights were recorded. An intraperitoneal glucose tolerance test (GTT) evaluated glycemic control in adulthood. As expected, Hf-Lf mice showed sex-specific weight gain and impaired glucose clearance compared to Chow mice (Figures 1B–1D). Consistent with increased tolerance to Hf-Lf-induced obesity that is specific to females, Hf-Lf female mice weighed less and showed a similar glucose clearance response to Chow males, even after six weeks of Hf-Lf feeding (Figures 1B–1D).

We next examined whether the sex-specific weight gain and glucose intolerance caused by the Hf-Lf diet affected diurnal variations in the gut microbiota differently in female and male mice. We collected cecal luminal contents from female and male mice assigned to either a Chow or Hf-Lf diet and collected samples every 4 h for 24 h. We then analyzed the microbiota in these samples using 16S rRNA marker gene sequencing and applied cosinor analysis to identify sex-specific rhythms in microbiota.[50] Our analysis revealed that 54 out of 293 (~17%) taxa showed oscillations in Chow females, and 46 out of 306 (~15%) taxa did so in Chow males (all *p*s < 0.05 by Cosinor test). Only 14 taxa exhibited similar patterns in both Chow female and male mice (Figure 1E, and see Table S1). In Hf-Lf mice, the number of rhythmic taxa decreased to ~4% and ~6.5% in females and males, respectively. Analysis of microbial acrophases, defined as the peak relative abundance of each taxon, revealed that the distribution of acrophases was localized to two time periods in Chow females: zeitgeber time ZT12 to ZT18, and ZT0 to ZT4 (where ZT0 is lights on and ZT12 is lights off). In contrast, acrophase distribution in Chow males extended across multiple time points (Figure 1E). Hf-Lf feeding disrupted the sex-specific distribution of acrophases present in Chow mice (Figure 1F), indicating that diet may play a role in influencing the phase distribution of oscillating microbiota in a sex-specific manner.

We then sought to identify how diet influences oscillations of specific taxa at the phylum and genus level in female and male mice. At the phylum level, the relative abundance of Bacteroidota, Firmicutes, Verrucomicrobiota, and Deferribacterota showed significant variation at ZT12 and ZT16 in Chow-fed female and male mice (Figure 1G).[27] Hf-Lf reduced the relative abundance of Firmicutes in both sexes, while Hf-Lf males showed a sex-specific expansion of Desulfobacterota during the behaviorally inactive phase (ZT0 and ZT12). This expansion was replaced by a bloom in the relative abundance of Bacteroidota, Proteobacteria, and Verrucomicrobiota during the behaviorally active phase (ZT16 and ZT20). These sex- and diet-specific effects were similarly detected at the genus level and influenced community alpha diversity, as measured by the Shannon Diversity Index (Figures 1H–1J).

Analysis at the genus level revealed additional sex-specific effects of diet on diurnal variation of microbiota composition (Figure 1G; and see Table S1). *Butyricicoccus*, a well-characterized butyrate producer, showed similar rhythmicity in Chow-fed males and females, with peak abundance around ZT16 (Figure 1K). *Segmented Filamentous Bacteria* showed sex-specific rhythmicity, with peak abundance occurring in females prior to males (ZT12 vs. ZT16, respectively) (Figure 1M). The relative abundance of *Mucispirillum* showed sex-specific rhythmicity in Chow-fed mice, with peak abundance in males at ZT20. *Prevotellaceae* UCG 001 showed sex-specific rhythmicity in Chow-fed mice, whereby relative abundance was in anti-phase in Chow-fed males and females (Figure 1L). *Alistipes* showed a Chow-fed male-specific increase during the behaviorally inactive phase but not in Chow-fed females. *Lactobacillus* showed peak abundance during the light phase, with Chow-fed females showing a higher overall abundance of this taxon. The relative abundance of *Muribaculaceae* (formerly S24-7) was stable across the time of day in Chow-fed males and females (all Cosinor *ps* > 0.05). Rhythmicity in *Butyricicoccus*, *Prevotellaceae* UCG 001, and *Segmented Filamentous Bacteria* was abolished in Hf-Lf female and male mice, suggesting that feeding rhythms and dietary factors within the Chow diet synergize to entrain rhythms of these taxa (Cosinor *ps* > 0.05) (Figures 1K–1M).

Loss of oscillations in the relative abundance of microbiota occurred concomitantly with a sex-specific gain of rhythm in Hf-Lf mice. Hf-Lf females gained rhythmicity in the relative abundance of *Blautia* and *Bilophila* compared with Hf-Lf males and Chow mice (Cosinor *ps* < 0.05) (Figures 1N and 1O). Hf-Lf males showed a gain of rhythmicity in the relative abundance of *Bacteroides*, *Akkermansia*, and *Desulfovibrio* compared to the other mice (Cosinor *ps* < 0.05) (Figures 1P–1R). Our results suggest that nutrients derived from diets that vary in carbohydrates, fat, and soluble fiber may exert sex-specific effects on diurnal variations in microbial structure, diversity, and composition within the cecal luminal contents of mice.

Diet drives sex-specific circadian rhythms in predicted microbial functional pathways

Sex differences in diurnal variation of microbiota composition suggest that core metabolic functions of the microbiome may also vary depending on the time of day. We conducted a gut metabolic modules (GMM) analysis to determine whether sex-specific oscillations in microbial community composition reflect changes in predicted microbial functional pathways. These modules represent a set of manually curated references of metabolic pathways reported to occur in the gut microbiome.[51] Twenty-seven out of 92 (29%) GMMs showed diurnal variation in Chow females, while only 3 out of 92 (3%) GMMs showed significant diurnal rhythms in males (Cosinor analysis, $p < 0.05$) (Figure 2A, and see Table S2).

Consistent with the notion that dietary-derived factors entrain diurnal variations of specific taxa, gut metabolic modules that oscillated in Chow mice were abolished in Hf-Lf mice. Cosinor analysis detected that 1 out of 90 (0.01%) GMMs gained diurnal variation in Hf-Lf females, while 31 out of 94 (32%) GMMs gained rhythms in Hf-Lf males (Figures 2A and 2C). Our analysis also revealed sex-specific effects of diet on rhythmic GMMs (Figure 2B). For instance, modules representing the synthesis and conversion of primary microbial metabolites, such as formate, butyrate, acetate, and propionate, showed significant oscillations in Chow females but not males (Figures 2D–2G). These GMMs remained constitutively high in Hf-Lf females and males regardless of the time of day. Moreover, Chow females and Hf-Lf males showed an overlap in 7 rhythmic GMMs, including processes involved in sulfate reduction and mucin degradation, which is consistent with the bloom

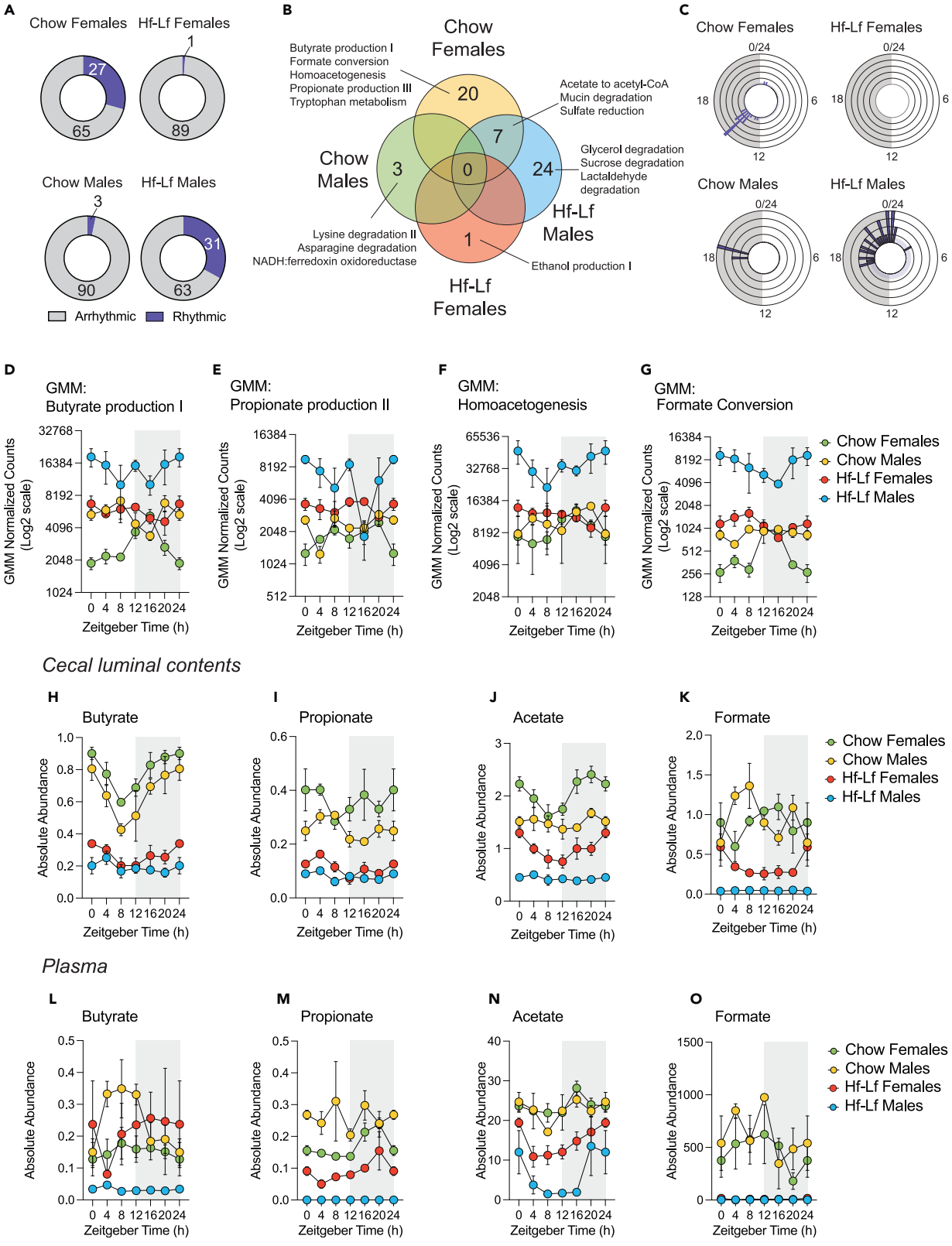
A
Chow Females
Hf-Lf Females
27
65
1
89
Chow Males
Hf-Lf Males
3
90
31
63
Arrhythmic
Rhythmic
B
Chow Females
Chow Males
Hf-Lf Males
Hf-Lf Females
Butyrate production I
Formate conversion
Homoacetogenesis
Propionate production III
Tryptophan metabolism
20
Acetate to acetyl-CoA
Mucin degradation
Sulfate reduction
7
Glycerol degradation
Sucrose degradation
Lactaldehyde degradation
24
3
0
Lysine degradation II
Asparagine degradation
NADH:ferredoxin oxidoreductase
1
Ethanol production I
C
Chow Females
Hf-Lf Females
Chow Males
Hf-Lf Males
0/24
6
12
18
D
GMM: Butyrate production I
E
GMM: Propionate production II
F
GMM: Homoacetogenesis
G
GMM: Formate Conversion
GMM Normalized Counts (Log2 scale)
Zeitgeber Time (h)
Chow Females
Chow Males
Hf-Lf Females
Hf-Lf Males
Cecal luminal contents
H
Butyrate
I
Propionate
J
Acetate
K
Formate
Absolute Abundance
Plasma
L
Butyrate
M
Propionate
N
Acetate
O
Formate

Figure 2. Diet modifies sex differences in diurnal rhythmicity of local and systemic availability of microbial metabolites

(A) Oscillation detection of non-rhythmic and rhythmic gut metabolic modules in the cecum of Chow and Hf-Lf mice using cosinor analysis (Cosinor $p < 0.05$).
(B) Venn diagram depicting differences in rhythmic gut metabolic modules between Chow and Hf-Lf mice.
(C) Rose plot depicting the distribution of maximum availability of rhythmic gut metabolic modules between Chow and Hf-Lf mice.
(D) Abundance of the gut metabolic module: butyrate production I shows sex-specific rhythmicity (Cosinor analysis, Chow females $p < 0.001$; Chow males $p = 0.257$; Hf-Lf females $p = 0.74$; Hf-Lf males $p = 0.303$).
(E) Abundance of the gut metabolic module: propionate production II shows sex-specific rhythmicity (Cosinor analysis, Chow females $p = 0.021$; Chow males $p = 0.433$; Hf-Lf females $p = 0.98$; Hf-Lf males $p = 0.18$).
(F) Abundance of the gut metabolic module: homoacetogenesis shows sex-specific rhythmicity (Cosinor analysis, Chow females $p < 0.01$; Chow males $p = 0.549$; Hf-Lf females $p = 0.44$; Hf-Lf males $p = 0.11$).
(G) Abundance of the gut metabolic module: formate conversion shows sex-specific rhythmicity (Cosinor analysis, Chow females $p < 0.001$; Chow males $p = 0.372$; Hf-Lf females $p = 0.17$; Hf-Lf males $p = 0.12$).
(H) Availability of butyrate in cecal lumen (Cosinor analysis, Chow females $p < 0.001$; Chow males $p = 0.372$; Hf-Lf females $p = 0.014$; Hf-Lf males $p = 0.36$).
(I) Availability of propionate in cecal lumen (Cosinor analysis, Chow females $p = 0.43$; Chow males $p = 0.037$; Hf-Lf females $p = 0.014$]3; Hf-Lf males $p = 0.12$).
(J) Availability of acetate in cecal lumen (Cosinor analysis, Chow females $p = 0.0006$; Chow males $p = 0.41$; Hf-Lf females $p = 0.006$; Hf-Lf males $p = 0.35$).
(K) Availability of formate in cecal lumen (Cosinor analysis, Chow females $p = 0.3$; Chow males $p = 0.16$; Hf-Lf females $p = 0.026$; Hf-Lf males $p = 0.79$).
(L) Availability of butyrate in plasma (Cosinor analysis, Chow females $p = 0.52$; Chow males $p = 0.0027$; Hf-Lf females $p = 0.57$; Hf-Lf males $p = 0.119$).
(M) Availability of propionate in plasma (Cosinor analysis, Chow females $p = 0.004$; Chow males $p = 0.98$; Hf-Lf females $p = 0.036$; Hf-Lf males $p = 0.117$).
(N) Availability of acetate in plasma (Cosinor analysis, Chow females $p = 0.35$; Chow males $p = 0.047$; Hf-Lf females $p = 0.008$; Hf-Lf males $p = 0.015$).
(O) Availability of formate in plasma (Cosinor analysis, Chow females $p = 0.077$; Chow males $p = 0.26$; Hf-Lf females $p = 0.014$; Hf-Lf males $p = 0.99$). Three murine-pathogen-free C57Bl/6NTac females and males were used for each condition, totaling 36 males and 36 females. Acrophases were calculated by cosinor analysis (period = 24 h). Full cosinor analysis in Tables S2 and S3. Data is represented as mean ± SEM.

in *Desulfovibrio* and Akkermansia observed in Hf-Lf males (see Figures 1Q and 1R). The GMM ethanol production showed diurnal variation in Hf-Lf females, consistent with earlier work showing that microbial communities shaped by a Hf-Lf diet exhibit an increased capacity for ethanol production.[52]

Diet shapes sex differences in the local and systemic availability of microbial-derived metabolites

As our GMM analyses revealed sex- and diet-specific differences in the functional potential of microbial pathways involved in the synthesis and conversion of microbial metabolites short-chain fatty acids (SCFAs), we next confirmed whether GMM oscillations reflected diurnal variations in the availability of SCFAs in the cecum and plasma.[53,54] SCFAs are derived from bacterial fermentation of dietary fiber and function as dynamic regulators of host physiology, such as regulating metabolic processes, constraining inflammation, controlling neural circuits involved in feeding and satiety, and regulating gene expression via histone post-translational modifications and inhibition of histone deacetylase activity.[55–57] To measure SCFAs, plasma and luminal cecal contents were collected every 4 h during a 24-h period from three female and male mice per time point. We used LC-MS/MS to measure the absolute quantification of the SCFAs formate, acetate, propionate, butyrate, valerate, and hexanoate. Valerate and hexanoate fell below our level of detection in this assay. As cecal weight differed across the day in males and females, we normalized cecal SCFA absolute quantities per gram body weight to control for sex differences in cecal SCFA concentration that may be attributed to baseline sexual dimorphism in mouse body weight (see Figure S1). Plasma SCFA absolute quantities were reported as a concentration (μg/mL) based on volume and thus do not change with body weight.[58]

As predicted by the GMM analysis, the diurnal variation in cecal luminal SCFA availability differed in a diet- and sex-specific manner (see Table S3). Chow females showed diurnal variations in the availability of cecal butyrate and acetate, and Chow males in cecal butyrate and propionate availability (Cosinor *p*s < 0.05) (Figures 2H–2J; and see Table S3). Formate was available in equal quantities across the day in Chow female and male cecum (Figure 2K). Hf-Lf feeding reduced the absolute concentration of butyrate, acetate, propionate, and formate relative to Chow mice, suggesting that excess dietary fat, loss of dietary fiber, or a combination of both affects SCFA availability (Figures 2H–2K). Despite this reduction in cecal SCFA output and amplitude, Hf-Lf mice maintained diurnal variations in SCFA availability in a sex-specific manner. For instance, Hf-Lf females preserved rhythmicity in cecal butyrate and acetate and gained rhythms in cecal propionate, while Hf-Lf males lost rhythmicity in cecal butyrate and propionate (Figures 2H–2K, and see Table S3). We replicate earlier work showing loss of diurnal variations in cecal butyrate in male mice[18] and now show that this previously observed effect is specific to male mice.

We analyzed plasma and examined how diurnal variations in cecal luminal SCFA availability influence circulating SCFA levels. Propionate was the only SCFA to show diurnal availability in the plasma of Chow females, while acetate and butyrate showed rhythmicity in the plasma of males (Figures 2L–2O; and see Table S2). Interestingly, in Chow males, the maximum availability of cecal butyrate was ZT21.5, and the maximum availability of plasma butyrate was ZT8.5 (Figures 2H and 2L; and see Table S3).[59] Although not significant, a similar trend was observed for propionate, whereby the maximum availability of cecal propionate was ZT23.5, and the maximum availability of plasma butyrate was ZT4.3 (Figures 2I and 2M; and see Table S3). Our reconstruction of SCFA suggests a ~12 h period from cecal-derived butyrate to plasma and provides a high-resolution timescale by which specific SCFAs become systemically availability to affect host physiological functions, including regulation of host gene expression, metabolism, and immune function.[23]

Like cecal SCFA availability, Hf-Lf feeding altered diurnal variation in butyrate, propionate, acetate, and formate availability in a sex-specific manner (Figures 2L–2O). Although Hf-Lf reduced absolute abundance in all SCFAs, Hf-Lf females preserved rhythmicity in plasma acetate and propionate, while Hf-Lf males maintained rhythmicity in plasma acetate and butyrate (Figures 2L and 2N, and see Table S3). As acetate

can be synthesized from various diet- and microbiota-independent processes,[60] it is thus not surprising that diurnal variations in systemic availability of acetate remain intact in Hf-Lf mice.

Lastly, we examined whether sex differences in diurnal variations of cecal and plasma SCFA availability depend on the microbiome. We collected whole ceca and plasma from germ-free female and male mice at ZT6, ZT10, ZT14, and ZT18. Diurnal variations in acetate, butyrate, and propionate availability in the cecum and plasma were abolished, and no differences between germ-free female and male mice were detected (see Figure S2). These results confirm that sex differences in diurnal variations in local and systemic SCFA availability are microbiome dependent. Moreover, host genetics and housing conditions also have strong effects on the magnitude of sex differences in mice.[61–63] To determine whether our observed sex differences in diurnal rhythms in microbiota and metabolites may reflect a generalizable pattern in commonly used laboratory mice, we repeated these experiments with BALB/c mice reared in a different animal housing facility. We observed similar sex differences in cecal weight and diurnal rhythms in cecal availability of SCFAs in Chow-fed BALB/c female and male mice (see Figure S3). Our integrated analytical approach identified sex differences in circadian rhythms of microbial structure, composition, predicted metabolic function, and output. The magnitude of sex differences in SCFA availability changed across the day. Furthermore, we show that various dietary factors, such as the diversity of carbohydrate sources, the presence or absence of soluble fibers, and the amount of saturated fats, determine sex-specific rhythms.

Gut microbiota are required for sex-specific circadian rhythms in host gene expression

Diurnal fluctuations in microbial metabolite availability affect gene expression patterns in host tissues.[64–66] This led us to hypothesize that our observed sex differences in the circadian rhythms of gut microbiota and microbial metabolites regulate gene expression of sex-specific cyclic genes within the intestinal tract. We collected small intestinal ileum segments from three female and male Chow-fed conventionalized (CV) and germ-free (GF) mice per time point across a 24-h period. CV females exhibited diurnal rhythms in 3961 transcripts (~24%) compared with 296 rhythmic transcripts (2%) in males ($p < 0.05$ by Cosinor test) (Figure 3A, and see Table S4). Analyses of acrophases revealed sex-specific distribution patterns in the maximum expression of cyclic genes. CV females exhibited a higher number of genes peaking between ZT8 to ZT12 and ZT16 to ZT20, while CV males showed a higher number of genes peaking between ZT2 to ZT6 and ZT12 to ZT18 (Figure 3B). Sex differences in the onset and acrophase of feeding have been observed, with females beginning to consume food ~4 h earlier than males.[67] This may suggest that phase shifts in gene expression reflect sex differences in the synchronization of feeding rhythms and microbiota, but further testing is needed to confirm these interactions. CV females and males also showed similar oscillations in only 66 genes, confirming sex differences in intestinal circadian gene expression (Figure 3C). The sex difference in the number of rhythmic genes and distribution of peak gene expression was abolished in GF mice (Figure 3A). GF females and males showed similar oscillations in 179 genes, indicating that a cluster of genes oscillated in a sex-specific manner in the absence of a microbiome (Figure 3B). *Pigv*, a gene that encodes a mannosyltransferase enzyme involved in the biosynthesis of glycosylphosphatidylinositol (*Gpi*), is the only non-sex-specific cyclic gene independent of microbiome status (Figure 3C). Defects in *Gpi* biosynthesis can lead to severe morbidity and mortality,[68] highlighting the importance of maintaining rhythmicity independent of sex and a microbiome. Thus, *Gpi* serves as a potential candidate gene to further investigate underlying microbiome-independent mechanisms that govern circadian rhythms.

We next investigated whether sex-specific rhythmic gene expression is associated with transcriptional networks and functional pathways using Gene Ontology-based overrepresentation analysis (with all pathways having a false discovery rate (FDR) < 0.05). Our analysis revealed sex-specific differences in transcriptional pathways involved in metabolism and immunity between CV and GF mice (Figure 3D, and see Table S5). CV female mice exhibited enrichment in pathways involved in intestinal absorption, fatty acid metabolism, cholesterol transport and biosynthesis, gluconeogenesis, immunoglobulin production, and mucosal immune response. In contrast, CV males showed enrichment in pathways involved in response to glucose, leptin, and insulin. GF mice did not show enrichment for these biological processes. Specifically, genes enriched in these pathways, including solute carrier family 4 member 1 (*Slac5a1/Slgt1*), free fatty acid receptor 2 (*Gpr42/Ffar2*), CD36 molecule (*Cd36*), leptin (*Lep*), leptin receptor (*Lepr*), insulin receptor substrate 1 (*Irs1*), glucagon-like peptide 1 receptor (*Glp1r*), Ezrin (*Ezr*), and fatty acid binding protein 2 (*Fabp2*) showed cyclicity. This cyclicity was abolished in GF mice (see Figures S4A–S4H). Our results build upon earlier work showing that microbial-derived signals are necessary for generating oscillations in genes involved in intestinal metabolism and immunity.[12,13] Here, we extend these findings to show that the microbiome is required for generating sex-specific circadian rhythms in intestinal gene expression patterns.

Dietary factors impact circadian rhythms in host gene expression in a sex-specific manner

We next examined whether microbiome-dependent expression of genes involved in metabolism, nutrient uptake, and immunity are influenced by dietary factors.[12,13,17,18,20,69] We investigated the effect of the Hf-Lf diet on cycling genes in the intestinal tract of female and male mice, comparing them to Chow females and males. Hf-Lf females had fewer rhythmic transcripts (~28% vs. ~4%), while Hf-Lf males had more (~7% vs. ~2%-) compared to the Chow mice (Figure 4A; and see Table S6). The increase in rhythmic genes in Hf-Lf males is likely related to the high degree of inter-sample variability across ZT collection time points in Chow males, which was reduced upon switching to the Hf-Lf diet, as observed in previous studies.[48,49] Analysis of acrophase distribution shows that the primary loss of rhythmic transcripts occurred during ZT18 to ZT24 in Hf-Lf females compared with Chow females (Figure 4B). Hf-Lf males showed a phase advance (~4 h) in the acrophase distribution of rhythmic genes, consistent with earlier work on the effects of hypercaloric and energy-dense feeding on circadian rhythms in the liver and adipose tissues[70,71] (Figure 4B).

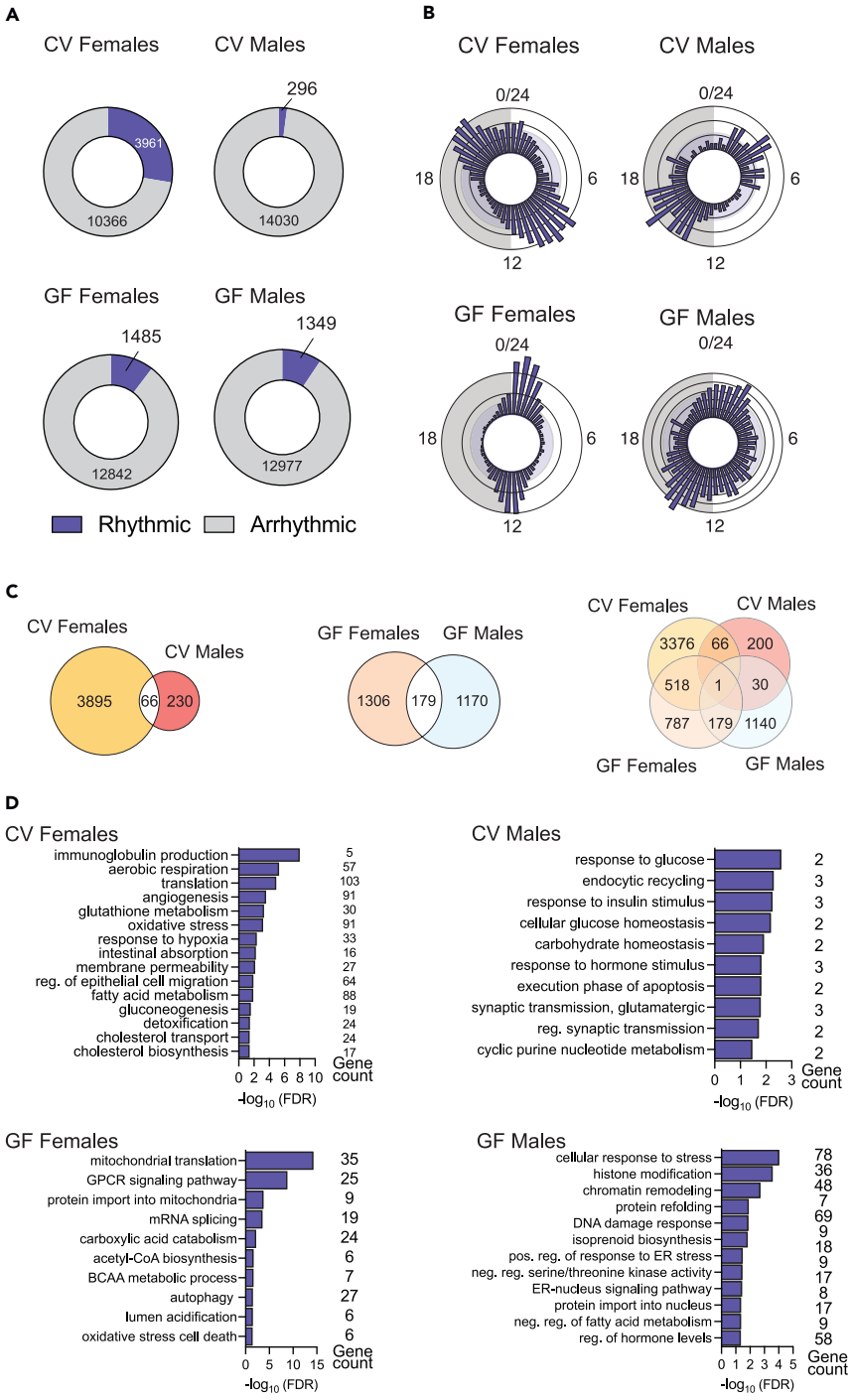

Figure 3. The intestinal microbiota is required for sex differences in diurnal rhythmicity of genes involved in immunity and metabolism

(A) Oscillation detection of non-rhythmic and rhythmic transcripts detected in the ileum of Chow diet conventionalized and germ-free female and male mice using cosinor analysis (Cosinor $p < 0.05$).

(B) Rose plot depicting the distribution of maximum expression of rhythmic genes in the ileum of Chow diet conventionalized and germ-free female and male mice.

(C) Venn diagram depicting differences in rhythmic gene expression in Chow diet conventionalized and germ-free female and male mice.

(D) PANTHER overrepresentation test of Gene Ontology using the Biological Process annotation dataset showing the enrichment of sex-specific pathways in the ileum of Chow diet conventionalized and germ-free female and male mice (Fisher's Exact Test, FDR <0.05). Three murine-pathogen-free C57Bl/6NTac females and males were used for each condition, totaling 30 males and 30 females. Acrophases were calculated by cosinor analysis (period = 24 h). Full cosinor and GO analysis in Tables S4 and S5, respectively.

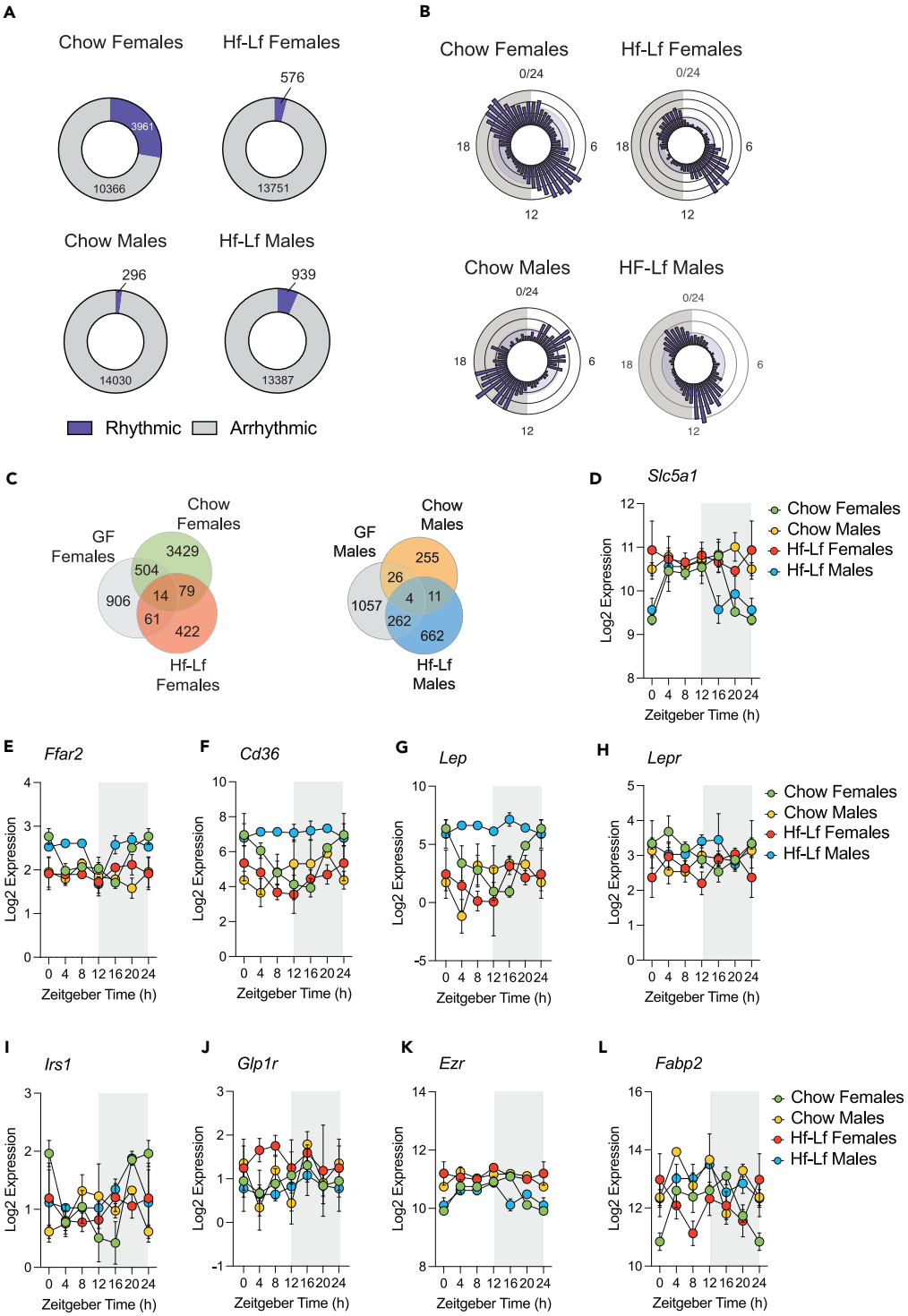

Figure 4. Diet modifies the magnitude of sex differences in diurnal rhythmicity of genes involved in metabolism

(A) Differences in non-rhythmic and rhythmic transcripts detected in the ileum of Chow and Hf-Lf female and male mice using cosinor analysis.

(B) Rose plot showing differences in acrophase distribution of genes in the adult ileum of Chow and Hf-Lf female and male mice.

(C) Venn diagram depicting differences in rhythmic gene expression in GF, Chow, and Hf-Lf female and male mice (all *p*s < 0.05 using Cosinor).

(D) Barplot depicting differences in diurnal variations in sodium-dependent glucose transporter (*Slc5a1*) gene expression in Chow and Hf-Lf female and male mice (Cosinor analysis, Chow females p = 0.014; Chow males p = 0.61; Hf-Lf females p = 0.93; Hf-Lf males p = 0.035).

Figure 4. *Continued*

(E) Barplot depicting differences in diurnal variations in free fatty acid receptor 2 (*Ffar2*) gene expression in Chow and Hf-Lf female and male mice (Cosinor analysis, Chow females p = 0.010; Chow males p = 0.51; Hf-Lf females p = 0.52; Hf-Lf males p = 0.15).

(F) Barplot depicting differences in diurnal variations in the CD36 molecule (*Cd36*) gene expression in Chow and Hf-Lf female and male mice (Cosinor analysis, Chow females p = 0.0009; Chow males p = 0.09; Hf-Lf females p = 0.21; Hf-Lf males p = 0.90).

(G) Barplot depicting differences in diurnal variations in leptin (*Lep*) gene expression in Chow and Hf-Lf female and male mice (Cosinor analysis, Chow females p = 0.0014; Chow males p = 0.13; Hf-Lf females p = 0.37; Hf-Lf males p = 0.63).

(H) Bar plot depicting differences in diurnal variations in leptin receptor (*Lepr*) gene expression in Chow and Hf-Lf female and male mice (Cosinor analysis, Chow females p = 0.004; Chow males p = 0.65; Hf-Lf females p = 0.37; Hf-Lf males p = 0.90).

(I) Barplot depicting differences in diurnal variations in insulin receptor substrate 1 (*Irs1*) gene expression in Chow and Hf-Lf female and male mice (Cosinor analysis, Chow females p = 0.011; Chow males p = 0.45; Hf-Lf females p = 0.72; Hf-Lf males p = 0.26).

(J) Barplot depicting differences in diurnal variations in glucagon-like peptide 1 receptor (*Glp1r*) gene expression in Chow and Hf-Lf female and male mice (Cosinor analysis, Chow females p = 0.63; Chow males p = 0.46; Hf-Lf females p = 0.79; Hf-Lf males p = 0.71).

(K) Barplot depicting differences in diurnal variations in Ezrin (*Ezr*) gene expression in Chow and Hf-Lf female and male mice (Cosinor analysis, Chow females p = 0.003; Chow males p = 0.45; Hf-Lf females p = 0.87; Hf-Lf males p = 0.15).

(L) Barplot depicting differences in diurnal variations in fatty-acid binding protein 2 (*Fabp2*) gene expression in Chow and Hf-Lf female and male mice (Cosinor analysis, Chow females p = 0.031; Chow males p = 0.65; Hf-Lf females p = 0.68; Hf-Lf males p = 0.27). Three murine-pathogen-free C57Bl/6NTac females and males were used for each condition, totaling 36 males and 36 females. Acrophases were calculated by cosinor analysis (period = 24 h). Full cosinor analysis in Table S6. Threshold for the cosinor test was set to $p < 0.05$.

Further, a comparison of GF, Chow, and Hf-Lf mice revealed sex-specific effects of diet and the microbiome on oscillating genes (Figure 4C). Fourteen genes were shared among all females, and four were shared among all males, representing a putative set of sex-specific oscillating genes independent of diet and the microbiome. Hf-Lf females gained rhythmicity in 422 genes, and Hf-Lf males in 662 genes (Figure 4C). As Hf-Lf feeding is known to alter the trafficking of metabolites across the intestine, we next examined candidate genes involved in intestinal nutrient absorption and transport that were identified in our comparison between CV and GF mice (see Figures S4A–S4H). Hf-Lf mice maintained sex-specific oscillations in these genes, albeit with different amplitudes. Hf-Lf feeding resulted in constitutively high expression of *Ffar2*, *Cd36*, and *Lep* in Hf-Lf males compared to chow males *and* chow females. The magnitude of the difference was greater when compared to Hf-Lf females (Figures 4E–4G, see Figures S5B–S5D). *Glp1r* was constitutively expressed in Hf-Lf females relative to Chow females and Chow males. The magnitude of the difference was again greater when compared to Hf-Lf males (Figure 4J). There was no difference in the expression of these genes between Chow males and females, although the amplitudes differed across the day (see Figure S6). The sustained upregulation of genes involved in glycemic control, lipid and fatty acid transport, and leptin signaling may suggest sex-specific metabolic adaptations to Hf-Lf feeding in the intestine.[29,42] Consistent with this, the Gene Ontology overrepresentation analysis (FDR <0.05) revealed that Hf-Lf males showed enrichment in gene pathways involved in lipid synthesis and storage, fatty acid metabolism, and response to insulin stimulus. Conversely, Hf-Lf females showed no enrichment in these pathways but a significant enrichment in gene pathways involved in mRNA metabolic processing (Table S7).

Finally, to confirm the circadian origin of the microbial rhythmicity, we evaluated the rhythmicity of ileal clock genes *Bmal1*, *Clock*, *Per1*, *Per2*, *Cry1*, and *Cry2* (see Figures S7A–S7F). We observed sex-specific circadian rhythms in gene expression patterns of the intestinal circadian clock genes. The results build upon earlier work showing that intestinal clock genes drive circadian microbiota composition[72] and further confirm that microbial diurnal rhythms are rooted in host intrinsic circadian mechanisms. Switching animals to the Hf-Lf diet changed the rhythmic expression of these clock genes in a sex-specific manner. This arrhythmicity in internal clock genes is reflected in alterations to the microbiome and microbial metabolites. These results demonstrate that diet modulates microbial rhythms and that arrhythmicity in intestinal clock genes impacts host metabolic functioning.

DISCUSSION

Sex differences in metabolic functions are crucial for life-long health. Disruption of these processes is associated with sex-specific risk for metabolic, immune, and neural disorders.[6] The gut microbiome is thought to play a critical role in meeting the divergent metabolic and immunologic demands of females and males.[8,9] Further, microbial communities show significant shifts across the time of day, and disruption to these circadian rhythms is associated with an increased risk for metabolic dysfunction and inflammation.[14,22,23,26,73] Although circadian disruption is often linked to sex-specific health outcomes, studies on circadian rhythms, the microbiome, and health outcomes commonly use only male mice or collapse both sexes into one experimental condition.[32] To address this knowledge gap, we investigated whether the microbiome is necessary to maintain sex differences in metabolism and transcriptional landscape within the intestinal tract across the time of day. Additionally, we examined the sex-specific effect of diet on these host-microbe interactions.

Here, we show that the relative abundance of gut microbiota fluctuates across time of day in a sex-specific manner. Our analyses focused on the cecal luminal microbiota because of its essential role in producing key microbial substrates important for metabolism.[74] Consistent with earlier studies examining the fecal microbiota,[27] we observed significant sex differences in the diurnal rhythms in the microbiota diversity, composition, and gut metabolic modules. These sex differences were not uniform across the day; instead, the magnitude of the difference between females and males depended on the time of day. Indeed, sex differences in feeding have been previously observed, with female mice beginning to consume food 4 h earlier than males and being driven by sex hormones.[67] Additionally, male mice on high-fat diets have disrupted diurnal feeding patterns and consume twice as many calories in the light periods.[30] Thus, we expected feeding patterns to

differ in a diet and sex-specific manner. While this study did not directly look at feeding patterns, our acrophase analysis of rhythmic transcripts suggests that gene expression phase shifts reflect sex differences in the synchronization of feeding rhythms. For instance, the relative abundance of *Segmented Filamentous Bacteria* (SFB) was higher in females at ZT12 (lights off), and males caught up 4 h later by ZT16. This rhythmic abundance in SFB drives diurnal rhythms in the expression of antimicrobial peptides as an anticipatory cue for food and exposure to exogenous microbiota during the behaviorally active phase.[11] Considering these observations, our results suggest that sex differences in SFB abundance may reflect sex differences in feeding rhythms, but added testing is needed to confirm this observation. Indeed, a recent report showed that females begin to eat about 2 h before lights off, resulting in an earlier onset and peak of the feeding rhythm and a phase advancement in overall host-microbe interactions.[67] Given the unique and context-specific ability of SFB to both exacerbate and protect against specific autoimmune-related pathologies in mice through alterations to host metabolism and immunity, the possible relationship between sex differences in diurnal variations of SFB, metabolism, immunity, and predisposition to disease warrants further exploration. We also observed sex-specific effects on the microbiome during the behaviorally inactive phase. The relative abundance of *Alistipes* and *Prevotellaceae UCG 001* is increased early in the behaviorally inactive phase in males but not females, while both sexes showed an increased abundance of *Lactobacillus*.

The diurnal variation in the relative abundance of cecal luminal microbiota also influenced oscillations of microbial metabolites in the cecum and plasma. We observed a peak in the relative abundance of *Butyricicoccus*, which preceded the peak availability of butyrate in the cecum, followed by the peak availability of plasma butyrate 6 h later. While these analyses reconstruct some sex-specific oscillations in microbiota and microbial metabolites, the present work remains an underestimate of all oscillating metabolites, given that the microbiome produces tens of thousands of metabolites. Incorporating time-of-day effects on microbiome-metabolite interactions will likely reveal novel epigenetic, metabolic, and immune associations involved in sex-specific health and disease. Diurnal fluctuations in the microbiome and microbial metabolites are associated with sex-specific oscillations in ileal transcriptional networks. Unlike males, females showed stepwise changes in the transcriptional networks across the day, showing time-of-day shifts from pathways involved in defense mechanisms to cholesterol and lipid absorption and epigenetic processes. These distinct shifts in transcriptional networks may reflect how physiological processes in the intestinal tract are partitioned over the day. Sex differences in host gene expression patterns are abolished in germ-free mice, suggesting that oscillations in microbiota and microbial metabolites are necessary for the distinct transcriptional landscape of the female and male ileum.

Our results raise a central question about the evolutionary origins of sex differences in host-microbe interactions. Life history theory posits that evolutionary pressures shape the timing of life events in males and females.[75–78] This theory focuses explicitly on defining age schedules of growth, fertility, senescence, and mortality.[75–78] As individuals grow and reproduce, they acquire increasing energy to balance the demands of their homeostatic processes and reproduction. Thus, the timing of such life events depends on resource and energy substrate availability.[75,77–81] From the perspective of life history trade-offs, individuals cannot continuously support all biological functions at all times of the day as the energy costs are too high. Circadian rhythms may thus enable individuals to partition and prioritize energy allocation toward life-history events relative to predictable fluctuations in environmental conditions, such as daily fluctuations in food availability.[82] Recent efforts to integrate the microbiome into life history evolution propose that the composition and function of microbial communities set the pace and timing of life history transitions.[83,84] This idea is supported by reports showing that abrupt changes to microbial composition and function coincide with the changes in energy allocations required to transition across development, reproduction, and senescence.[10,85,86] Our work suggests that sex-specific circadian rhythms in host-microbe interactions represent one proximate mechanism that links environmental factors such as food availability to the unique energy demands of female and male life histories.

Another important question concerns the role of diet and the energetic costs needed for the sex-specific maintenance of diurnal fluctuations in microbes, microbial metabolites, and host genes. Earlier work highlighted that the nutritional composition of diets and the timing of specific nutrient intake entrain peripheral circadian rhythms in rodents and humans.[87] For instance, shifting animals from a low-protein, high-carbohydrate diet to a high-protein, low-carbohydrate diet changed the rhythmic expression of genes involved in gluconeogenesis in the mouse kidney and liver.[88] Switching human participants from a high-carbohydrate and low-fat diet to an isoenergetic diet composed of low-carbohydrate and high-fat increased the amplitude of rhythmic genes involved in inflammation and metabolism.[89] One extrapolation of this work is that the timing of food intake and the nutritional composition of diets function as entrainment signals for host-microbe interactions. Microbial communities prefer distinct dietary components, including protein, fiber, lactate, and urea.[90] Proportional changes to the accessibility of nutrients result in an ecological advantage for bacteria supplied with their preferred substrate.[90] From this perspective, it is unsurprising that transitioning mice from chow to a high-fat, low-fiber diet eliminated circadian rhythms that are entrained by the consumption of a Chow diet. Sex-specific loss of rhythmicity occurred in microbiota and microbial metabolites that utilize soluble fiber. This may suggest that the parallel sex-specific loss of rhythmicity in host genes is related to decreased availability of soluble fiber and warrants further study.[53]

Conversely, the consumption of a high-fat, low-fiber diet (Hf-Lf) initiated rhythmic oscillations of microbiota in a sex-specific manner. At the microbiome level, Hf-Lf females showed a gain of rhythm in *Blautia* and *Bilophila*, taxa that favor dietary lipids for growth and expansion and are associated with visceral fat accumulation.[91,92] Hf-Lf males showed gained rhythmicity in the relative abundance of *Bacteroides*, *Akkermansia*, and *Desulfovibrio*. This sex-specific gain of rhythmicity correlated with parallel sex differences in gut metabolic module rhythmicity, whereby Hf-Lf male-specific gain of rhythmicity in *Akkermansia* and *Bacteroides* reflected gut metabolic modules that map to the functional potential of these taxa, including mucin degradation, sulfate reduction, and simple sugar degradation.[93,94] This suggests that the gain of rhythmicity in community composition may be directly related to microbial functional potential and output. Further, we replicated earlier

work showing a gain of rhythm in the hydrogen sulfide-producing taxa *Desulfovibrio*,[18] and we showed that this is a male-specific effect. Female and male mice show distinct metabolic adaptations to Hf-Lf feeding, whereby females, but not males, increase energy expenditure, increase insulin sensitivity, maintain activity levels, and decrease the respiratory quotient, which is suggestive of a greater ability to utilize fat from the diet as an alternative source of energy.[29,42] Our transcriptomic analysis showing upregulation of genes involved in sensing dietary lipids, intestinal lipid uptake, and transport in male but not female mice may indicate that dysregulation of these genes contributes to weight gain. Indeed, increased intestinal *Cd36, Ffar2,* and *Lep* expression is associated with an increased body mass index.[95] Identifying the underlying mechanisms that maintain the rhythmicity of dietary lipid-sensing genes in Hf-Lf females may provide novel targets to reinstate rhythmicity and resistance to diet-induced obesity and metabolic syndrome in males.

Perspective and significance

Our studies provide evidence for sex-specific circadian rhythms in the microbial, metabolite, and transcriptional capacity of the intestinal tract under *ad libitium* feeding conditions, indicating sex differences in host-microbe interactions are time-of-day dependent. Our observations also suggest that chronic circadian disruption caused by a high-fat, low-fiber diet affects the synchronization between the microbiome, microbial metabolites, and host transcriptome in a sex-specific manner. We show that sex-specific risk for diet-induced metabolic dysfunction involves, at least in part, host-microbe circadian rhythms. Our reconstruction of sex differences in the onset, acrophase, and amplitude of circadian rhythms can guide the selection of appropriate data collection times. Given the significant effects of the microbiome on health and disease trajectories,[96–101] further experiments are needed to investigate how disruption to these processes influences sex-specific disease risk.

These findings demonstrating the interactions between diet, circadian rhythms, and the gut microbiota have practical considerations for studying sex differences in preclinical and clinical settings, as the timing of data collection may influence the detection of sex differences in homeostatic and disease processes.[102,103] Difficulty in translating preclinical findings to human populations may be related to the lack of incorporation of circadian rhythms in study designs,[37] which may contribute to the large interindividual variability observed in microbial composition.[104] Our results highlight the importance of considering time-related frameworks in study design and data collection when studying host-microbe interactions. Frameworks that synchronize pharmaceutical and nutritional interventions to the host-microbe endogenous sex-specific circadian system will likely maximize host health outcomes in metabolic and immune-related diseases.

Conclusions

Overall, our data highlights the importance of studying sex differences in circadian rhythms across the microbiome, metabolites, and the expression of host genes. A better understanding of these fundamental processes can offer novel insight into diseases that exhibit significant sex bias in onset, severity, and treatment outcomes.

Limitations of the study

One limitation of our study is that the impact of gonadal hormones on sex difference in microbial circadian rhythms was not assessed. Gonadal hormones, such as estradiol and testosterone, play a significant role in sex differences, including protection and resistance to diet-induced obesity in female mice.[105,106] While our results reveal lower variance in females, indicating a limited impact of the estrous cycle on our findings, we did not track the estrus cycle across the 24-h period. Therefore, we cannot exclude the role of gonadal hormone status in the interaction between microbial circadian rhythms, diet, host gene expression, and sex differences in metabolism. To obtain additional information on hormone-mediated effects on microbial circadian rhythms and host metabolism, we recommend using standard methods to track the estrous cycle, manipulate gonadal hormones, and employ the four core genotypes mouse model.[67,99,100]

STAR★METHODS

Detailed methods are provided in the online version of this paper and include the following:

- KEY RESOURCES TABLE
- RESOURCE AVAILABILITY
  - Lead contact
  - Materials availability
  - Data and code availability
- EXPERIMENTAL MODEL AND STUDY PARTICIPANT DETAILS
  - Confirmation of germ-free status
- METHOD DETAILS
  - Glucose tolerance test
  - Cecal luminal content DNA extraction and 16S rRNA marker gene sequencing
  - Ileum RNA extraction and preparation for RNA-seq
  - Quantification of 3NP-short chain fatty acids
  - Analysis of targeted metabolomics data

- Processing and analysis of 16S rRNA marker gene sequencing data
- Processing and analysis of bulk RNA-seq data
- Gut metabolic modules

- QUANTIFICATION AND STATISTICAL ANALYSIS

SUPPLEMENTAL INFORMATION

Supplemental information can be found online at https://doi.org/10.1016/j.isci.2023.107999.

ACKNOWLEDGMENTS

This work is supported by funding from the Eunice Kennedy Shriver National Institute of Child Health and Human Development grants T32HD087194 (PI: SKM) Pilot Project from P50HD096723 (PI: EJ), the National Institute of Diabetes and Digestive and Kidney Diseases grant K01DK1121734 (PI: EJ), a Magee Auxiliary Research Scholars Award (PI: EJ) and Start-Up funds from Magee-Womens Research Institute. The Health Sciences Metabolomics and Lipidomics Core is supported by grant S10OD023402 (PI: SGW). We acknowledge Timothy Hand, Jacob DeSchepper, and Javonn Musgrove in the University of Pittsburgh Gnotobiotic Animal Studies Facility for technical assistance with circadian collections of germ-free mouse tissues. We acknowledge Will MacDonald in the Children's Hospital of Pittsburgh Health Sciences Sequencing Core for technical assistance with bulk RNA sequencing on the NextSeq 2000. We acknowledge Heather Evers, Cheyenne Miller, Heather Seiple, and Aaron Siegel in the Magee-Womens Research Institute animal facility for technical assistance in the care of mice. We acknowledge the University of Pittsburgh Center for Research Computing through the resources provided. Specifically, this work used the HTC cluster, supported by NIH award number S10OD028483.

AUTHOR CONTRIBUTIONS

Conceptualization, S.K.M., J.P.G., K.E.M., and E.J.; methodology, investigation, and validation, S.K.M., S.J.M., J.P.G., J.K.B., A.L., and A.J.K; formal analysis, S.K.M., A.K., and E.J.; resources, C.A.M., S.G.W., and E.J.; data curation, S.K.M., J.P.G., A.K., and E.J.; writing – original draft, S.K.M., J.P.G., and E.J., writing – reviewing and editing, S.K.M., S.G.W., K.E.M., J.P.G., and E.J.; supervision, E.J.; project administration, J.P.G and E.J.; funding acquisition, E.J.

DECLARATION OF INTERESTS

The authors have no competing interests.

INCLUSION AND DIVERSITY

One or more of the authors of this paper self-identifies as an underrepresented ethnic minority in their field of research or within their geographical location. One or more of the authors of this paper self-identifies as a member of the LGBTQIA+ community. One or more of the authors of this paper received support from a program designed to increase minority representation in their field of research. While citing references scientifically relevant for this work, we also actively worked to promote gender balance in our reference list.

Received: May 23, 2023
Revised: August 19, 2023
Accepted: September 18, 2023
Published: September 22, 2023

REFERENCES

1. Becker, J.B., Berkley, K.J., Geary, N., Hampson, E., Herman, J.P., and Young, E. (2007). Sex Differences in the Brain: From Genes to Behavior (Oxford University Press).
2. Geary, D.C. (2010). Male, Female: The Evolution of Human Sex Differences, 2nd ed (American Psychological Association). https://doi.org/10.1037/12072-000.
3. Geary, D.C. (2016). Evolution of sex differences in trait- and age-specific vulnerabilities. Perspect. Psychol. Sci. *11*, 855–876. https://doi.org/10.1177/1745691616650677.
4. Korstanje, R., Li, R., Howard, T., Kelmenson, P., Marshall, J., Paigen, B., and Churchill, G. (2004). Influence of sex and diet on quantitative trait loci for HDL cholesterol levels in an SM/J by NZB/BINJ intercross population. J. Lipid Res. *45*, 881–888. https://doi.org/10.1194/jlr.M300460-JLR200.
5. Mackay, T.F.C. (2004). The genetic architecture of quantitative traits: lessons from Drosophila. Curr. Opin. Genet. Dev. *14*, 253–257. https://doi.org/10.1016/j.gde.2004.04.003.
6. Ober, C., Loisel, D.A., and Gilad, Y. (2008). Sex-specific genetic architecture of human disease. Nat. Rev. Genet. *9*, 911–922. https://doi.org/10.1038/nrg2415.
7. Ueno, T., Tremblay, J., Kunes, J., Zicha, J., Dobesova, Z., Pausova, Z., Deng, A.Y., Sun, Y.-L., Jacob, H.J., and Hamet, P. (2004). Rat model of familial combined hyperlipidemia as a result of comparative mapping. Physiol. Genomics *17*, 38–47. https://doi.org/10.1152/physiolgenomics.00043.2003.
8. Jaggar, M., Rea, K., Spichak, S., Dinan, T.G., and Cryan, J.F. (2020). You've got male: Sex and the microbiota-gut-brain axis across the lifespan. Front. Neuroendocrinol. *56*, 100815. https://doi.org/10.1016/j.yfrne.2019.100815.
9. Jašarević, E., Morrison, K.E., and Bale, T.L. (2016). Sex differences in the gut microbiome–brain axis across the lifespan. Philos. Trans. R. Soc. Lond. B Biol. Sci. *371*, 20150122. https://doi.org/10.1098/rstb.2015.0122.
10. Yatsunenko, T., Rey, F.E., Manary, M.J., Trehan, I., Dominguez-Bello, M.G., Contreras, M., Magris, M., Hidalgo, G., Baldassano, R.N., Anokhin, A.P., et al. (2012). Human gut microbiome viewed across age and geography. Nature *486*,

222–227. https://doi.org/10.1038/nature11053.
11. Brooks, J.F., Behrendt, C.L., Ruhn, K.A., Lee, S., Raj, P., Takahashi, J.S., and Hooper, L.V. (2021). The microbiota coordinates diurnal rhythms in innate immunity with the circadian clock. Cell *184*, 4154–4167.e12. https://doi.org/10.1016/j.cell.2021.07.001.
12. Kuang, Z., Wang, Y., Li, Y., Ye, C., Ruhn, K.A., Behrendt, C.L., Olson, E.N., and Hooper, L.V. (2019). The intestinal microbiota programs diurnal rhythms in host metabolism through histone deacetylase 3. Science *365*, 1428–1434. https://doi.org/10.1126/science.aaw3134.
13. Wang, Y., Kuang, Z., Yu, X., Ruhn, K.A., Kubo, M., and Hooper, L.V. (2017). The intestinal microbiota regulates body composition through NFIL3 and the circadian clock. Science *357*, 912–916. https://doi.org/10.1126/science.aan0677.
14. Alvarez, Y., Glotfelty, L.G., Blank, N., Dohnalová, L., and Thaiss, C.A. (2020). The Microbiome as a Circadian Coordinator of Metabolism. Endocrinology *161*, bqaa059. https://doi.org/10.1210/endocr/bqaa059.
15. Heinemann, M., Ratiner, K., and Elinav, E. (2021). Basic Biology of Rhythms and the Microbiome. In Circadian Rhythms in Bacteria and Microbiomes, C.H. Johnson and M.J. Rust, eds. (Springer International Publishing), pp. 317–328. https://doi.org/10.1007/978-3-030-72158-9_16.
16. Altaha, B., Heddes, M., Pilorz, V., Niu, Y., Gorbunova, E., Gigl, M., Kleigrewe, K., Oster, H., Haller, D., and Kiessling, S. (2022). Genetic and environmental circadian disruption induce metabolic impairment through changes in the gut microbiome. Preprint at bioRxiv. https://doi.org/10.1101/2022.07.27.501612.
17. Dantas Machado, A.C., Brown, S.D., Lingaraju, A., Sivaganesh, V., Martino, C., Chaix, A., Zhao, P., Pinto, A.F.M., Chang, M.W., Richter, R.A., et al. (2022). Diet and feeding pattern modulate diurnal dynamics of the ileal microbiome and transcriptome. Cell Rep. *40*, 111008. https://doi.org/10.1016/j.celrep.2022.111008.
18. Leone, V., Gibbons, S.M., Martinez, K., Hutchison, A.L., Huang, E.Y., Cham, C.M., Pierre, J.F., Heneghan, A.F., Nadimpalli, A., Hubert, N., et al. (2015). Effects of Diurnal Variation of Gut Microbes and High-Fat Feeding on Host Circadian Clock Function and Metabolism. Cell Host Microbe *17*, 681–689. https://doi.org/10.1016/j.chom.2015.03.006.
19. Thaiss, C.A., Zeevi, D., Levy, M., Zilberman-Schapira, G., Suez, J., Tengeler, A.C., Abramson, L., Katz, M.N., Korem, T., Zmora, N., et al. (2014). Transkingdom Control of Microbiota Diurnal Oscillations Promotes Metabolic Homeostasis. Cell *159*, 514–529. https://doi.org/10.1016/j.cell.2014.09.048.
20. Zarrinpar, A., Chaix, A., Yooseph, S., and Panda, S. (2014). Diet and feeding pattern affect the diurnal dynamics of the gut microbiome. Cell Metab. *20*, 1006–1017.
21. Zarrinpar, A., Chaix, A., Xu, Z.Z., Chang, M.W., Marotz, C.A., Saghatelian, A., Knight, R., and Panda, S. (2018). Antibiotic-induced microbiome depletion alters metabolic homeostasis by affecting gut signaling and colonic metabolism. Nat. Commun. *9*, 2872. https://doi.org/10.1038/s41467-018-05336-9.
22. Brooks, J.F., and Hooper, L.V. (2020). Interactions among microbes, the immune system, and the circadian clock. Semin. Immunopathol. *42*, 697–708. https://doi.org/10.1007/s00281-020-00820-1.
23. Choi, H., Rao, M.C., and Chang, E.B. (2021). Gut microbiota as a transducer of dietary cues to regulate host circadian rhythms and metabolism. Nat. Rev. Gastroenterol. Hepatol. *18*, 679–689. https://doi.org/10.1038/s41575-021-00452-2.
24. Frazier, K., and Chang, E.B. (2020). Intersection of the Gut Microbiome and Circadian Rhythms in Metabolism. Trends Endocrinol. Metab. *31*, 25–36. https://doi.org/10.1016/j.tem.2019.08.013.
25. Penny, H.A., Domingues, R.G., Krauss, M.Z., Melo-Gonzalez, F., Lawson, M.A.E., Dickson, S., Parkinson, J., Hurry, M., Purse, C., Jegham, E., et al. (2022). Rhythmicity of intestinal IgA responses confers oscillatory commensal microbiota mutualism. Sci. Immunol. *7*, eabk2541. https://doi.org/10.1126/sciimmunol.abk2541.
26. Zheng, D., Ratiner, K., and Elinav, E. (2020). Circadian Influences of Diet on the Microbiome and Immunity. Trends Immunol. *41*, 512–530. https://doi.org/10.1016/j.it.2020.04.005.
27. Liang, X., Bushman, F.D., and FitzGerald, G.A. (2015). Rhythmicity of the intestinal microbiota is regulated by gender and the host circadian clock. Proc. Natl. Acad. Sci. USA *112*, 10479–10484. https://doi.org/10.1073/pnas.1501305112.
28. Weger, B.D., Gobet, C., Yeung, J., Martin, E., Jimenez, S., Betrisey, B., Foata, F., Berger, B., Balvay, A., Foussier, A., et al. (2019). The Mouse Microbiome Is Required for Sex-Specific Diurnal Rhythms of Gene Expression and Metabolism. Cell Metab. *29*, 362–382.e8. https://doi.org/10.1016/j.cmet.2018.09.023.
29. Casimiro, I., Stull, N.D., Tersey, S.A., and Mirmira, R.G. (2021). Phenotypic sexual dimorphism in response to dietary fat manipulation in C57BL/6J mice. J. Diabetes Complications *35*, 107795. https://doi.org/10.1016/j.jdiacomp.2020.107795.
30. Kohsaka, A., Laposky, A.D., Ramsey, K.M., Estrada, C., Joshu, C., Kobayashi, Y., Turek, F.W., and Bass, J. (2007). High-fat diet disrupts behavioral and molecular circadian rhythms in mice. Cell Metab. *6*, 414–421. https://doi.org/10.1016/j.cmet.2007.09.006.
31. Hatori, M., Vollmers, C., Zarrinpar, A., DiTacchio, L., Bushong, E.A., Gill, S., Leblanc, M., Chaix, A., Joens, M., Fitzpatrick, J.A.J., et al. (2012). Time-Restricted Feeding without Reducing Caloric Intake Prevents Metabolic Diseases in Mice Fed a High-Fat Diet. Cell Metab. *15*, 848–860. https://doi.org/10.1016/j.cmet.2012.04.019.
32. Walton, J.C., Bumgarner, J.R., and Nelson, R.J. (2022). Sex Differences in Circadian Rhythms. Cold Spring Harb. Perspect. Biol. *14*, a039107. https://doi.org/10.1101/cshperspect.a039107.
33. Pettersson, U.S., Waldén, T.B., Carlsson, P.-O., Jansson, L., and Phillipson, M. (2012). Female mice are protected against high-fat diet induced metabolic syndrome and increase the regulatory T cell population in adipose tissue. PLoS One *7*, e46057. https://doi.org/10.1371/journal.pone.0046057.
34. Giles, D.A., Moreno-Fernandez, M.E., Stankiewicz, T.E., Graspeuntner, S., Cappelletti, M., Wu, D., Mukherjee, R., Chan, C.C., Lawson, M.J., Klarquist, J., et al. (2017). Thermoneutral housing exacerbates nonalcoholic fatty liver disease in mice and allows for sex-independent disease modeling. Nat. Med. *23*, 829–838. https://doi.org/10.1038/nm.4346.
35. Avgerinos, K.I., Spyrou, N., Mantzoros, C.S., and Dalamaga, M. (2019). Obesity and cancer risk: emerging biological mechanisms and perspectives. Metabolism *92*, 121–135. https://doi.org/10.1016/j.metabol.2018.11.001.
36. McKenzie, C., Tan, J., Macia, L., and Mackay, C.R. (2017). The nutrition-gut microbiome-physiology axis and allergic diseases. Immunol. Rev. *278*, 277–295. https://doi.org/10.1111/imr.12556.
37. Gutierrez Lopez, D.E., Lashinger, L.M., Weinstock, G.M., and Bray, M.S. (2021). Circadian rhythms and the gut microbiome synchronize the host's metabolic response to diet. Cell Metab. *33*, 873–887. https://doi.org/10.1016/j.cmet.2021.03.015.
38. Buettner, R., Schölmerich, J., and Bollheimer, L.C. (2007). High-fat diets: modeling the metabolic disorders of human obesity in rodents. Obesity *15*, 798–808. https://doi.org/10.1038/oby.2007.608.
39. Cani, P.D., Amar, J., Iglesias, M.A., Poggi, M., Knauf, C., Bastelica, D., Neyrinck, A.M., Fava, F., Tuohy, K.M., Chabo, C., et al. (2007). Metabolic endotoxemia initiates obesity and insulin resistance. Diabetes *56*, 1761–1772. https://doi.org/10.2337/db06-1491.
40. Sampey, B.P., Vanhoose, A.M., Winfield, H.M., Freemerman, A.J., Muehlbauer, M.J., Fueger, P.T., Newgard, C.B., and Makowski, L. (2011). Cafeteria diet is a robust model of human metabolic syndrome with liver and adipose inflammation: comparison to high-fat diet. Obesity *19*, 1109–1117. https://doi.org/10.1038/oby.2011.18.
41. Cani, P.D., Bibiloni, R., Knauf, C., Waget, A., Neyrinck, A.M., Delzenne, N.M., and Burcelin, R. (2008). Changes in gut microbiota control metabolic endotoxemia-induced inflammation in high-fat diet–induced obesity and diabetes in mice. Diabetes *57*, 1470–1481.
42. Oraha, J., Enriquez, R.F., Herzog, H., and Lee, N.J. (2022). Sex-specific changes in metabolism during the transition from chow to high-fat diet feeding are abolished in response to dieting in C57BL/6J mice. Int. J. Obes. *46*, 1749–1758. https://doi.org/10.1038/s41366-022-01174-4.
43. Gohir, W., Kennedy, K.M., Wallace, J.G., Saoi, M., Bellissimo, C.J., Britz-McKibbin, P., Petrik, J.J., Surette, M.G., and Sloboda, D.M. (2019). High-fat diet intake modulates maternal intestinal adaptations to pregnancy and results in placental hypoxia, as well as altered fetal gut barrier proteins and immune markers. J. Physiol. *597*, 3029–3051. https://doi.org/10.1113/JP277353.
44. Jašarević, E., Hill, E.M., Kane, P.J., Rutt, L., Gyles, T., Folts, L., Rock, K.D., Howard, C.D., Morrison, K.E., Ravel, J., and Bale, T.L. (2021). The composition of human vaginal microbiota transferred at birth affects offspring health in a mouse model. Nat. Commun. *12*, 6289. https://doi.org/10.1038/s41467-021-26634-9.
45. Chassaing, B., Miles-Brown, J., Pellizzon, M., Ulman, E., Ricci, M., Zhang, L., Patterson, A.D., Vijay-Kumar, M., and Gewirtz, A.T. (2015). Lack of soluble fiber drives diet-induced adiposity in mice. APSselect *309*, G528–G541. https://doi.org/10.1152/ajpgi.00172.2015@apsselect.2015.2.issue-11.

46. Dalby, M.J., Ross, A.W., Walker, A.W., and Morgan, P.J. (2017). Dietary Uncoupling of Gut Microbiota and Energy Harvesting from Obesity and Glucose Tolerance in Mice. Cell Rep. *21*, 1521–1533. https://doi.org/10.1016/j.celrep.2017.10.056.
47. Morrison, K.E., Jašarević, E., Howard, C.D., and Bale, T.L. (2020). It's the fiber, not the fat: significant effects of dietary challenge on the gut microbiome. Microbiome *8*, 15. https://doi.org/10.1186/s40168-020-0791-6.
48. Pellizzon, M.A., and Ricci, M.R. (2018). The common use of improper control diets in diet-induced metabolic disease research confounds data interpretation: the fiber factor. Nutr. Metab. *15*, 3. https://doi.org/10.1186/s12986-018-0243-5.
49. Pellizzon, M.A., and Ricci, M.R. (2020). Choice of Laboratory Rodent Diet May Confound Data Interpretation and Reproducibility. Curr. Dev. Nutr. *4*, nzaa031. https://doi.org/10.1093/cdn/nzaa031.
50. Cornelissen, G. (2014). Cosinor-based rhythmometry. Theor. Biol. Med. Model. *11*, 16. https://doi.org/10.1186/1742-4682-11-16.
51. Vieira-Silva, S., Falony, G., Darzi, Y., Lima-Mendez, G., Garcia Yunta, R., Okuda, S., Vandeputte, D., Valles-Colomer, M., Hildebrand, F., Chaffron, S., and Raes, J. (2016). Species–function relationships shape ecological properties of the human gut microbiome. Nat. Microbiol. *1*, 16088. https://doi.org/10.1038/nmicrobiol.2016.88.
52. Singh, R.P., Halaka, D.A., Hayouka, Z., and Tirosh, O. (2020). High-Fat Diet Induced Alteration of Mice Microbiota and the Functional Ability to Utilize Fructooligosaccharide for Ethanol Production. Front. Cell. Infect. Microbiol. *10*, 376.
53. Geirnaert, A., Steyaert, A., Eeckhaut, V., Debruyne, B., Arends, J.B.A., Van Immerseel, F., Boon, N., and Van de Wiele, T. (2014). Butyricicoccus pullicaecorum, a butyrate producer with probiotic potential, is intrinsically tolerant to stomach and small intestine conditions. Anaerobe *30*, 70–74. https://doi.org/10.1016/j.anaerobe.2014.08.010.
54. Segers, A., Desmet, L., Thijs, T., Verbeke, K., Tack, J., and Depoortere, I. (2019). The circadian clock regulates the diurnal levels of microbial short-chain fatty acids and their rhythmic effects on colon contractility in mice. Acta Physiol. *225*, e13193. https://doi.org/10.1111/apha.13193.
55. Chang, P.V., Hao, L., Offermanns, S., and Medzhitov, R. (2014). The microbial metabolite butyrate regulates intestinal macrophage function via histone deacetylase inhibition. Proc. Natl. Acad. Sci. USA *111*, 2247–2252. https://doi.org/10.1073/pnas.1322269111.
56. De Vadder, F., Kovatcheva-Datchary, P., Goncalves, D., Vinera, J., Zitoun, C., Duchampt, A., Bäckhed, F., and Mithieux, G. (2014). Microbiota-Generated Metabolites Promote Metabolic Benefits via Gut-Brain Neural Circuits. Cell *156*, 84–96. https://doi.org/10.1016/j.cell.2013.12.016.
57. Smith, P.M., Howitt, M.R., Panikov, N., Michaud, M., Gallini, C.A., Bohlooly-Y, M., Glickman, J.N., and Garrett, W.S. (2013). The microbial metabolites, short chain fatty acids, regulate colonic Treg cell homeostasis. Science *341*, 569–573. https://doi.org/10.1126/science.1241165.
58. Han, J., Lin, K., Sequeira, C., and Borchers, C.H. (2015). An isotope-labeled chemical derivatization method for the quantitation of short-chain fatty acids in human feces by liquid chromatography–tandem mass spectrometry. Anal. Chim. Acta *854*, 86–94. https://doi.org/10.1016/j.aca.2014.11.015.
59. Boets, E., Gomand, S.V., Deroover, L., Preston, T., Vermeulen, K., De Preter, V., Hamer, H.M., Van den Mooter, G., De Vuyst, L., Courtin, C.M., et al. (2017). Systemic availability and metabolism of colonic-derived short-chain fatty acids in healthy subjects: a stable isotope study. J. Physiol. *595*, 541–555. https://doi.org/10.1113/JP272613.
60. Bose, S., Ramesh, V., and Locasale, J.W. (2019). Acetate Metabolism in Physiology, Cancer, and Beyond. Trends Cell Biol. *29*, 695–703. https://doi.org/10.1016/j.tcb.2019.05.005.
61. Jonasson, Z. (2005). Meta-analysis of sex differences in rodent models of learning and memory: a review of behavioral and biological data. Neurosci. Biobehav. Rev. *28*, 811–825. https://doi.org/10.1016/j.neubiorev.2004.10.006.
62. Org, E., Mehrabian, M., Parks, B.W., Shipkova, P., Liu, X., Drake, T.A., and Lusis, A.J. (2016). Sex differences and hormonal effects on gut microbiota composition in mice. Gut Microb. *7*, 313–322. https://doi.org/10.1080/19490976.2016.1203502.
63. Võikar, V., Kõks, S., Vasar, E., and Rauvala, H. (2001). Strain and gender differences in the behavior of mouse lines commonly used in transgenic studies. Physiol. Behav. *72*, 271–281. https://doi.org/10.1016/S0031-9384(00)00405-4.
64. Grieneisen, L., Muehlbauer, A.L., and Blekhman, R. (2020). Microbial control of host gene regulation and the evolution of host–microbiome interactions in primates. Philos. Trans. R. Soc. Lond. B Biol. Sci. *375*, 20190598. https://doi.org/10.1098/rstb.2019.0598.
65. Richards, A.L., Burns, M.B., Alazizi, A., Barreiro, L.B., Pique-Regi, R., Blekhman, R., and Luca, F. (2016). Genetic and Transcriptional Analysis of Human Host Response to Healthy Gut Microbiota. mSystems *1*, e00067-16. https://doi.org/10.1128/mSystems.00067-16.
66. Richards, A.L., Muehlbauer, A.L., Alazizi, A., Burns, M.B., Findley, A., Messina, F., Gould, T.J., Cascardo, C., Pique-Regi, R., Blekhman, R., and Luca, F. (2019). Gut Microbiota Has a Widespread and Modifiable Effect on Host Gene Regulation. mSystems *4*, e00323-18. https://doi.org/10.1128/mSystems.00323-18.
67. Chen, X., Wang, L., Loh, D.H., Colwell, C.S., Taché, Y., Reue, K., and Arnold, A.P. (2015). Sex differences in diurnal rhythms of food intake in mice caused by gonadal hormones and complement of sex chromosomes. Horm. Behav. *75*, 55–63. https://doi.org/10.1016/j.yhbeh.2015.07.020.
68. Kinoshita, T. (2016). Glycosylphosphatidylinositol (GPI) Anchors: Biochemistry and Cell Biology: Introduction to a Thematic Review Series. J. Lipid Res. *57*, 4–5. https://doi.org/10.1194/jlr.E065417.
69. Whitt, J., Woo, V., Lee, P., Moncivaiz, J., Haberman, Y., Denson, L., Tso, P., and Alenghat, T. (2018). Disruption of Epithelial HDAC3 in Intestine Prevents Diet-Induced Obesity in Mice. Gastroenterology *155*, 501–513. https://doi.org/10.1053/j.gastro.2018.04.017.
70. Mendoza, J., Pévet, P., and Challet, E. (2008). High-fat feeding alters the clock synchronization to light. J. Physiol. *586*, 5901–5910. https://doi.org/10.1113/jphysiol.2008.159566.
71. Pendergast, J.S., Branecky, K.L., Yang, W., Ellacott, K.L.J., Niswender, K.D., and Yamazaki, S. (2013). High-fat diet acutely affects circadian organization and eating behavior. Eur. J. Neurosci. *37*, 1350–1356. https://doi.org/10.1111/ejn.12133.
72. Heddes, M., Altaha, B., Niu, Y., Reitmeier, S., Kleigrewe, K., Haller, D., and Kiessling, S. (2022). The intestinal clock drives the microbiome to maintain gastrointestinal homeostasis. Nat. Commun. *13*, 6068. https://doi.org/10.1038/s41467-022-33609-x.
73. Zarrinpar, A., Chaix, A., and Panda, S. (2016). Daily Eating Patterns and Their Impact on Health and Disease. Trends Endocrinol. Metab. *27*, 69–83. https://doi.org/10.1016/j.tem.2015.11.007.
74. Donaldson, G.P., Lee, S.M., and Mazmanian, S.K. (2016). Gut biogeography of the bacterial microbiota. Nat. Rev. Microbiol. *14*, 20–32. https://doi.org/10.1038/nrmicro3552.
75. Cole, L.C. (1954). The Population Consequences of Life History Phenomena. Q. Rev. Biol. *29*, 103–137. https://doi.org/10.1086/400074.
76. Hill, K., and Kaplan, H. (1999). Life History Traits in Humans: Theory and Empirical Studies. Annu. Rev. Anthropol. *28*, 397–430.
77. Partridge, L., and Harvey, P.H. (1988). The Ecological Context of Life History Evolution. Science *241*, 1449–1455. https://doi.org/10.1126/science.241.4872.1449.
78. Stearns, S.C. (1989). Trade-Offs in Life-History Evolution. Funct. Ecol. *3*, 259–268. https://doi.org/10.2307/2389364.
79. Charnov, E. (1993). Life History Invariants: Some Explorations of Symmetry in Evolutionary Ecology (Oxford University Press).
80. Roff, D. (1993). Evolution of Life Histories, First edition (Springer).
81. West-Eberhard, M.J. (1989). Phenotypic Plasticity and the Origins of Diversity. Annu. Rev. Ecol. Syst. *20*, 249–278.
82. Martinez-Bakker, M., and Helm, B. (2015). The influence of biological rhythms on host–parasite interactions. Trends Ecol. Evol. *30*, 314–326. https://doi.org/10.1016/j.tree.2015.03.012.
83. Metcalf, C.J.E., Henry, L.P., Rebolleda-Gómez, M., and Koskella, B. (2019). Why Evolve Reliance on the Microbiome for Timing of Ontogeny? mBio *10*, e01496-19. https://doi.org/10.1128/mBio.01496-19.
84. Turnbaugh, P.J., Ley, R.E., Mahowald, M.A., Magrini, V., Mardis, E.R., and Gordon, J.I. (2006). An obesity-associated gut microbiome with increased capacity for energy harvest. Nature *444*, 1027–1031. https://doi.org/10.1038/nature05414.
85. Al Nabhani, Z., Dulauroy, S., Marques, R., Cousu, C., Al Bounny, S., Déjardin, F., Sparwasser, T., Bérard, M., Cerf-Bensussan, N., and Eberl, G. (2019). A Weaning Reaction to Microbiota Is Required for Resistance to Immunopathologies in the Adult. Immunity *50*, 1276–1288.e5. https://doi.org/10.1016/j.immuni.2019.02.014.
86. Jašarević, E., Howard, C.D., Misic, A.M., Beiting, D.P., and Bale, T.L. (2017). Stress

during pregnancy alters temporal and spatial dynamics of the maternal and offspring microbiome in a sex-specific manner. Sci. Rep. *7*, 44182. https://doi.org/10.1038/srep44182.

87. Potter, G.D.M., Cade, J.E., Grant, P.J., and Hardie, L.J. (2016). Nutrition and the Circadian System. Br. J. Nutr. *116*, 434–442. https://doi.org/10.1017/S0007114516002117.
88. Oishi, K., Uchida, D., and Itoh, N. (2012). Low-Carbohydrate, High-Protein Diet Affects Rhythmic Expression of Gluconeogenic Regulatory and Circadian Clock Genes in Mouse Peripheral Tissues. Chronobiol. Int. *29*, 799–809. https://doi.org/10.3109/07420528.2012.699127.
89. Pivovarova, O., Jürchott, K., Rudovich, N., Hornemann, S., Ye, L., Möckel, S., Murahovschi, V., Kessler, K., Seltmann, A.-C., Maser-Gluth, C., et al. (2015). Changes of Dietary Fat and Carbohydrate Content Alter Central and Peripheral Clock in Humans. J. Clin. Endocrinol. Metab. *100*, 2291–2302. https://doi.org/10.1210/jc.2014-3868.
90. Zeng, X., Xing, X., Gupta, M., Keber, F.C., Lopez, J.G., Lee, Y.-C.J., Roichman, A., Wang, L., Neinast, M.D., Donia, M.S., et al. (2022). Gut bacterial nutrient preferences quantified in vivo. Cell *185*, 3441–3456.e19. https://doi.org/10.1016/j.cell.2022.07.020.
91. Natividad, J.M., Lamas, B., Pham, H.P., Michel, M.-L., Rainteau, D., Bridonneau, C., da Costa, G., van Hylckama Vlieg, J., Sovran, B., Chamignon, C., et al. (2018). Bilophila wadsworthia aggravates high fat diet induced metabolic dysfunctions in mice. Nat. Commun. *9*, 2802. https://doi.org/10.1038/s41467-018-05249-7.
92. Ozato, N., Saito, S., Yamaguchi, T., Katashima, M., Tokuda, I., Sawada, K., Katsuragi, Y., Kakuta, M., Imoto, S., Ihara, K., and Nakaji, S. (2019). Blautia genus associated with visceral fat accumulation in adults 20–76 years of age. npj Biofilms Microbiomes *5*, 28–29. https://doi.org/10.1038/s41522-019-0101-x.
93. Makki, K., Deehan, E.C., Walter, J., and Bäckhed, F. (2018). The Impact of Dietary Fiber on Gut Microbiota in Host Health and Disease. Cell Host Microbe *23*, 705–715. https://doi.org/10.1016/j.chom.2018.05.012.
94. Desai, M.S., Seekatz, A.M., Koropatkin, N.M., Kamada, N., Hickey, C.A., Wolter, M., Pudlo, N.A., Kitamoto, S., Terrapon, N., Muller, A., et al. (2016). A Dietary Fiber-Deprived Gut Microbiota Degrades the Colonic Mucus Barrier and Enhances Pathogen Susceptibility. Cell *167*, 1339–1353.e21. https://doi.org/10.1016/j.cell.2016.10.043.
95. Little, T.J., Isaacs, N.J., Young, R.L., Ott, R., Nguyen, N.Q., Rayner, C.K., Horowitz, M., and Feinle-Bisset, C. (2014). Characterization of duodenal expression and localization of fatty acid-sensing receptors in humans: relationships with body mass index. Am. J. Physiol. Gastrointest. Liver Physiol. *307*, G958–G967. https://doi.org/10.1152/ajpgi.00134.2014.
96. Belkaid, Y., and Hand, T.W. (2014). Role of the Microbiota in Immunity and Inflammation. Cell *157*, 121–141. https://doi.org/10.1016/j.cell.2014.03.011.
97. Collins, N., and Belkaid, Y. (2022). Control of immunity via nutritional interventions. Immunity *55*, 210–223. https://doi.org/10.1016/j.immuni.2022.01.004.
98. Helmink, B.A., Khan, M.A.W., Hermann, A., Gopalakrishnan, V., and Wargo, J.A. (2019). The microbiome, cancer, and cancer therapy. Nat. Med. *25*, 377–388. https://doi.org/10.1038/s41591-019-0377-7.
99. Kostic, A.D., Xavier, R.J., and Gevers, D. (2014). The Microbiome in Inflammatory Bowel Disease: Current Status and the Future Ahead. Gastroenterology *146*, 1489–1499. https://doi.org/10.1053/j.gastro.2014.02.009.
100. McDonald, B., and McCoy, K.D. (2019). Maternal microbiota in pregnancy and early life. Science *365*, 984–985. https://doi.org/10.1126/science.aay0618.
101. Round, J.L., and Mazmanian, S.K. (2009). The gut microbiota shapes intestinal immune responses during health and disease. Nat. Rev. Immunol. *9*, 313–323. https://doi.org/10.1038/nri2515.
102. Nelson, R.J., Bumgarner, J.R., Walker, W.H., and DeVries, A.C. (2021). Time-of-day as a critical biological variable. Neurosci. Biobehav. Rev. *127*, 740–746. https://doi.org/10.1016/j.neubiorev.2021.05.017.
103. Nelson, R.J., Bumgarner, J.R., Liu, J.A., Love, J.A., Meléndez-Fernández, O.H., Becker-Krail, D.D., Walker, W.H., Walton, J.C., DeVries, A.C., and Prendergast, B.J. (2022). Time of day as a critical variable in biology. BMC Biol. *20*, 142. https://doi.org/10.1186/s12915-022-01333-z.
104. Human Microbiome Project Consortium (2012). Structure, Function and Diversity of the Healthy Human Microbiome. Nature *486*, 207–214. https://doi.org/10.1038/nature11234.
105. Acharya, K.D., Graham, M., Raman, H., Parakoyi, A.E.R., Corcoran, A., Belete, M., Ramaswamy, B., Koul, S., Sachar, I., Derendorf, K., et al. (2023). Estradiol-mediated protection against high-fat diet induced anxiety and obesity is associated with changes in the gut microbiota in female mice. Sci. Rep. *13*, 4776. https://doi.org/10.1038/s41598-023-31783-6.
106. Acharya, K.D., Noh, H.L., Graham, M.E., Suk, S., Friedline, R.H., Gomez, C.C., Parakoyi, A.E.R., Chen, J., Kim, J.K., and Tetel, M.J. (2021). Distinct Changes in Gut Microbiota Are Associated with Estradiol-Mediated Protection from Diet-Induced Obesity in Female Mice. Metabolites *11*, 499. https://doi.org/10.3390/metabo11080499.
107. R Core Team (2022). R: A Language and Environment for Statistical Computing (R Foundation for Statistical Computing). https://www.R-project.org/.
108. Carlucci, M., Kriščiūnas, A., Li, H., Gibas, P., Koncevičius, K., Petronis, A., and Oh, G. (2019). DiscoRhythm: an easy-to-use web application and R package for discovering rhythmicity. Bioinformatics *36*, 1952–1954. https://doi.org/10.1093/bioinformatics/btz834.
109. Bolyen, E., Rideout, J.R., Dillon, M.R., Bokulich, N.A., Abnet, C.C., Al-Ghalith, G.A., Alexander, H., Alm, E.J., Arumugam, M., Asnicar, F., et al. (2019). Reproducible, interactive, scalable and extensible microbiome data science using QIIME 2. Nat. Biotechnol. *37*, 852–857. https://doi.org/10.1038/s41587-019-0209-9.
110. Callahan, B.J., McMurdie, P.J., Rosen, M.J., Han, A.W., Johnson, A.J.A., and Holmes, S.P. (2016). DADA2: High-resolution sample inference from Illumina amplicon data. Nat. Methods *13*, 581–583. https://doi.org/10.1038/nmeth.3869.
111. Quast, C., Pruesse, E., Yilmaz, P., Gerken, J., Schweer, T., Yarza, P., Peplies, J., and Glöckner, F.O. (2013). The SILVA ribosomal RNA gene database project: improved data processing and web-based tools. Nucleic Acids Res. *41*, D590–D596. https://doi.org/10.1093/nar/gks1219.
112. Dhariwal, A., Chong, J., Habib, S., King, I.L., Agellon, L.B., and Xia, J. (2017). MicrobiomeAnalyst: a web-based tool for comprehensive statistical, visual and meta-analysis of microbiome data. Nucleic Acids Res. *45*, W180–W188. https://doi.org/10.1093/nar/gkx295.
113. Bray, N.L., Pimentel, H., Melsted, P., and Pachter, L. (2016). Near-optimal probabilistic RNA-seq quantification. Nat. Biotechnol. *34*, 525–527. https://doi.org/10.1038/nbt.3519.
114. Robinson, M.D., McCarthy, D.J., and Smyth, G.K. (2010). edgeR: a Bioconductor package for differential expression analysis of digital gene expression data. Bioinformatics *26*, 139–140. https://doi.org/10.1093/bioinformatics/btp616.
115. Yu, G., Wang, L.-G., Han, Y., and He, Q.-Y. (2012). clusterProfiler: an R package for comparing biological themes among gene clusters. OMICS *16*, 284–287. https://doi.org/10.1089/omi.2011.0118.
116. Thomas, P.D., Ebert, D., Muruganujan, A., Mushayahama, T., Albou, L.-P., and Mi, H. (2022). PANTHER: Making genome-scale phylogenetics accessible to all. Protein Sci. *31*, 8–22. https://doi.org/10.1002/pro.4218.
117. Douglas, G.M., Maffei, V.J., Zaneveld, J.R., Yurgel, S.N., Brown, J.R., Taylor, C.M., Huttenhower, C., and Langille, M.G.I. (2020). PICRUSt2 for prediction of metagenome functions. Nat. Biotechnol. *38*, 685–688. https://doi.org/10.1038/s41587-020-0548-6.
118. Kanehisa, M., Goto, S., Sato, Y., Furumichi, M., and Tanabe, M. (2012). KEGG for integration and interpretation of large-scale molecular data sets. Nucleic Acids Res. *40*, D109–D114. https://doi.org/10.1093/nar/gkr988.
119. Valles-Colomer, M., Falony, G., Darzi, Y., Tigchelaar, E.F., Wang, J., Tito, R.Y., Schiweck, C., Kurilshikov, A., Joossens, M., Wijmenga, C., et al. (2019). The neuroactive potential of the human gut microbiota in quality of life and depression. Nat. Microbiol. *4*, 623–632. https://doi.org/10.1038/s41564-018-0337-x.

STAR★METHODS

KEY RESOURCES TABLE

REAGENT or RESOURCE	SOURCE	IDENTIFIER
Critical commercial assays		
MagAttract PowerMicrobiome DNA/RNA EP Kit	Qiagen	Cat. # 27500-4-EP
miRNeasy Mini Kit	Qiagen	Cat. # 217004
TruSeq Stranded mRNA Kit	Illumina	Cat. # 20020595
Agilent High Sensitivity D5000 ScreenTape Assay	Agilent	Cat. # 5067-5592
Agilent High Sensitivity RNA ScreenTape Assay	Agilent	Cat. # 5067-5579
Qubit RNA HS Assay Kit	ThermoFisher	Cat. #Q32852
Qubit dsDNA HS Assay Kit	ThermoFisher	Cat. #Q32851
Agencourt Ampure XP Beads	Beckman Coulter	Cat. # A63881
Illumina Stranded mRNA Prep, Ligation kit	Illumina	Cat. #20040534
IDT for Illumina RNA UD Indexes Set A	Illumina	Cat. #20040553
Nextera XT DNA Library Preparation Kit (96 samples)	Illumina	Cat. #FC-131-1096
Nextera XT Index Kit v2 Set A (96 indexes, 384 samples)	Illumina	Cat. #FC-131-2001
Deposited data		
mRNAseq FASTQ files	This paper	Accession: PRJNA1014373
16S rRNA FASTQ files	This paper	Accession: PRJNA1014373
Experimental models: Organisms/strains		
Mouse: C57BL/6NTac MPF	Taconic	Stock No: B6-MPF
Mouse: C57BL/6NTac GF	Taconic	Stock No: B6-GF
Mouse: BALB/c	In house	N/A
Oligonucleotides		
16S Amplicon PCR Forward Primer: 5′TCGTCGGCAGCGTCAGATGTGTATAAGAGACAGCCTACGGGNGGCWGCAG	Integrated DNA Technologies	N/A
16S Amplicon PCR Reverse Primer: 5′GTCTCGTGGGCTCGGAGATGTGTATAAGAGACAGGACTACHVGGGTATCTAATCC	Integrated DNA Technologies	N/A
Software and algorithms		
QIIME 2 Core 2022.2 DADA2		https://docs.qiime2.org/2022.8/install/
R version 4.1.0	R Core Team, 2021[107]	https://www.r-project.org/
RStudio version 1.2.5001	RStudio, Inc.	https://www.rstudio.com/
MicrobiomeAnalyst		https://www.microbiomeanalyst.ca/
Kallisto	Github	https://github.com/pachterlab/kallisto
tximport (version 3.4)		https://bioconductor.org/packages/release/bioc/html/tximport.html
edgeR		https://bioconductor.org/packages/release/bioc/html/edgeR.html
GOmixer		http://www.raeslab.org/software/gomixer.tar.gz
clusterProfiler		https://bioconductor.org/packages/release/bioc/html/clusterProfiler.html

(*Continued on next page*)

Continued

REAGENT or RESOURCE	SOURCE	IDENTIFIER
PantherDB		clusterProfiler https://bioconductor.org/packages/release/data/annotation/html/PANTHER.db.html
PICRUSt2		https://github.com/picrust/picrust2/releases
DiscoRhythm		https://bioconductor.org/packages/release/bioc/html/DiscoRhythm.htmlpanthrDB panther
GraphPad Prism		https://www.graphpad.com
Other		
PicoLab Mouse Diet 20 - chow	LabDiet	Cat. # 5058
High-Fat Low-Fiber Diet	Research Diets	Cat. #D12492
NIH #31M Rodent Diet	Envigo	Cat. # 7913

RESOURCE AVAILABILITY

Lead contact

Further information and requests for resources and reagents should be directed to and will be fulfilled by the lead contact, Eldin Jašarević (eldin.jasarevic@pitt.edu).

Materials availability

This study did not generate new reagents and all reagents were commercially purchased and used as received.

Data and code availability

- The RNA-seq and microbiota data generated in this study have been deposited in the NCBI SRA database under the Bioproject PRJNA1014373 (https://www.ncbi.nlm.nih.gov/bioproject/PRJNA1014373). All additional raw data and analysis outputs reported in this paper are shared as supplementary materials and any additional requests for data will be shared by the lead contact upon request without restrictions.
- This paper does not report original code.
- Any additional information required to reanalyze the data reported in this paper is available from the lead contact upon request.

EXPERIMENTAL MODEL AND STUDY PARTICIPANT DETAILS

All experiments were approved by the University of Pittsburgh and Magee-Womens Research Institute Institutional Animal Care and Use Committee and performed in accordance with the National Institutes of Health Animal Care and Use Guidelines. C57Bl/6N female and male mice from Taconic Biosciences (C57Bl/6NTac) arrived at the animal facility aged three weeks. All mice were single-housed and acclimated to housing conditions for at least one week before experimentation. All mice were maintained on a 12-h light/dark cycle (lights on 0600, zeitgeber time (ZT) 0; lights off 1800, ZT 12). Room temperature was maintained between 75–77°F and 40–60% humidity. An Onset HOBO MX2202 Wireless Temperature/Light Data Logger (HOBO Data Loggers, Wilmington, NC) was used to confirm light-dark photoperiod stability. *Ad libitum* access was provided to water and either a chow diet (NIH #31M Rodent Diet, Envigo; 23.0% protein, 59.0% carbohydrate, 18.0% fat, PicoLab Mouse Diet 20; 23.2% protein, 55.2% carbohydrate, 21.6% fat), or a high-fat low-fiber diet (Research Diets D12492; 20.0% protein, 20.0% carbohydrate, 60.0% fat. Germ-free mice were fed a chow diet (NIH #31M Rodent Diet, Envigo; 23.0% protein, 59.0% carbohydrate, 18.0% fat). For circadian collections, three mice from each condition from separate cages were euthanized, and plasma, ileum, cecum, and brain samples were during a 24 h period for each of the six time points on the zeitgeber timescale (ZT0, ZT4, ZT8, ZT12, ZT16, ZT20). Due to limitations in after-hours access to gnotobiotic facilities, circadian collections of germ-free mice occurred at four time points (ZT4, ZT8, ZT12, ZT16). Ileum and cecum samples were rapidly frozen on dry ice and stored at −80C until further processing.

Confirmation of germ-free status

The University of Pittsburgh Gnotobiotic Facility conducts quarterly screening for bacterial contamination in germ-free mice. Screening for the detection of bacterial contamination of mouse feces by aerobic and anaerobic bacteria includes bacterial culture and qPCR assays. Screens were negative on all assays from isolators within which germ-free mice for this study were housed prior to

the initiation of experiments and following the conclusion of the experiments. This confirms the germ-free status of mice used in these studies.

METHOD DETAILS

Glucose tolerance test

Glucose tolerance test was administered in 10-week-old mice. Food was removed at 0800 EST and mice were fasted for 6 h, upon which mice were injected intraperitoneally with 1 mg/kg BW of 0.3 g/mL glucose in saline at 1400 EST. Glucose readings were collected by tail blood at 0-, 15- 30-, 60-, and 120-min timepoints using the Contour Next Blood Glucose Monitoring System (Bayer Co, Germany).

Cecal luminal content DNA extraction and 16S rRNA marker gene sequencing

The MagAttract PowerMicrobiome DNA/RNA Kit (Qiagen) extracted genomic DNA from fifty milligrams of cecal luminal contents using bead-beating on a TissueLyser II (Qiagen), according to the manufacturer's instructions. 16S libraries were generated using a two-step PCR protocol. Amplicon PCR was performed as follows for amplification of the 16s rRNA V3-V4 region from cecal luminal contents: initial denaturation at 95°C for 3 min, followed by 25-cyles 95°C for 30 s, 55°C for 30 s, 72°C for 30 s, and a final extension at 72°C for 5 min. Resultant 16S V3-V4 amplicons were then purified using AMPure XP beads at a 0.8 ratio of beads to amplicon volume. Illumina Nextera XT v2 Index Primer 1 (N7xx) and Nextera XT v2 Index Primer 2 (S5xx) were index primers. Index PCR was performed as follows for amplification of the 16s rRNA V3-V4 region from cecal luminal contents: initial denaturation at 95°C for 3 min, followed by 8-cyles 95°C for 30 s, 55°C for 30 s, 72°C for 30 s, and a final extension at 72°C for 5 min. Results indexed libraries were cleaned up using AMPure XP beads at a 0.8 ratio of beads to the indexed library. The concentration of indexed libraries was quantified using a Qubit 4 fluorimeter, and library fragment size was quantified using an Agilent Tapestation 4200 with D5000 ScreenTapes. Libraries were normalized pooled, and a paired-end sequencing of pooled libraries was done on an Illumina iSeq 100 System using 2x150 bp run geometry in our laboratory.

Ileum RNA extraction and preparation for RNA-seq

Frozen tissue samples were homogenized in QIAzol Reagent (Qiagen) using a MiltenyiBiotec gentleMACS Octo Dissociator for 30s. RNA was isolated with Qiagen miRNeasy Mini Kits according to the manufacturer's instructions. RNA integrity was quantified on an Agilent Tapestation 4200 using TapeStation RNA ScreenTapes. All samples had an RIN score above 8. Sequencing libraries were prepared using Illumina Stranded mRNA prep, Ligation kits with IDT for Illumina RNA UD Indexes Set A, and Ligation index adapters. The concentration of indexed libraries was quantified using Qubit, and library fragment size was quantified using an Agilent Tapestation 4200 with D5000 ScreenTapes. Sequencing was performed on an Illumina NextSeq 2000 using P3 flow cells and 2x100 paired end-run geometry at the Health Sciences Sequencing Core at Children's Hospital of Pittsburgh. Sequencing was repeated twice on the same library pool to achieve sufficient resolution and minimize batch effects, producing an average of 30–60 million reads per sample.

Quantification of 3NP-short chain fatty acids

Cecal luminal contents were homogenized with 50% aqueous acetonitrile at a ratio of 1:15 vol: wt. 5 μg/mL Deuterated internal standards: (D2)-formate, (D4)-acetate, (D5)-butyrate, (D6)-propionate, (D2)-valerate and (D4)-hexanoate (CDN Isotopes, Quebec, Canada) were added. Samples were homogenized using a FastPrep-24 system (MP-Bio), with Matrix D at 60hz for 30 s, before being cleared of protein by centrifugation at 16,000xg. Plasma samples were cleared of protein using 4x volumes ice-cold 1:1 MeOH: EtOH with vortexing, followed by centrifugation at 16,000xg. 60μL cleared supernatants were collected and derivatized using 3-nitrophenylhydrazine. Each sample was mixed with 20 μL of 200 mM 3-nitrophenylhydrazine in 50% aqueous acetonitrile and 20 μL of 120 mM N-(3-dimethylaminopropyl)-N0-ethylcarbodiimide −6% pyridine solution in 50% aqueous acetonitrile. The mixture reacted at 60°C for 40 min, and the reaction was stopped with 0.45 mL of 50% acetonitrile. Derivatized samples were injected (50 μL) via a Thermo Vanquish UHPLC and separated over a reversed-phase Phenomenex Kinetex 150 mm × 2.1 mm 1.7μM particle C18 maintained at 55°C. For the 20-min LC gradient, the mobile phase consisted of solvent A (water/0.1% FA) and solvent B (ACN/0.1% FA). The gradient was 0-2 min 15% B, increased to 60%B over 10 min, continued increasing to 100%B over 1 min, held at 100%B for 3 min, and reequilibrated at 15%B for 4 min. The Thermo IDX tribrid mass spectrometer was operated in both positive ion mode, scanning in ddMS2 mode (2 μscans) from 75 to 1000 m/z at 120,000 resolutions with an AGC target of 2e5 for full scan, 2e4 for ms2 scans using HCD fragmentation at stepped 15,35,50 collision energies. The source ionization setting was 3.0 kV spray voltage respectively, for positive mode. Source gas parameters were 45 sheath gas, 12 auxiliary gas at 320°C, and 3 sweep gas. Calibration was performed before analysis using the PierceTM FlexMix Ion Calibration Solutions (Thermo Fisher Scientific). Integrated peak areas were then extracted manually using Quan Browser (Thermo Fisher Xcalibur ver. 2.7). SCFAs are reported as the area ratio of SCFA to the internal standard.[58]

Analysis of targeted metabolomics data

Oscillation of absolute or relative metabolite abundance and period of oscillation were detected using Cosinor analysis using the R package DiscoRhythm.[108] Metabolites with $p < 0.05$ over a 24-h oscillation period are reported.

Processing and analysis of 16S rRNA marker gene sequencing data

The sequences were demultiplexed on the BaseSpace Sequence Hub using the bcl2fastq2 conversion software (version 2.2.0.) and analyzed using QIIME 2 (version 2022.2)[109] microbiome bioinformatics platform. Quality control on the resulting demultiplexed forward fastq files was performed using DADA2[110] denoise-single function trimming 33 bp of the primer sequence. A Naive Bayes feature classifier was trained using SILVA reference sequences[111] with the q2-feature-classifier for taxonomic analysis. The average count per sample was 27,611, with the maximum count per sample at 42,407 and the minimum count at 10,939. Statistical and meta-analysis of the data was conducted using MicrobiomeAnalyst.[112] Data filtering was set to include features where 20% of its values contain a minimum of four counts. In addition, features that exhibit low variance across treatment conditions are unlikely to be associated with treatment conditions. Therefore, the variance was measured by the interquartile range and removed at 10%. Data were normalized by using a trimmed mean of M-values. Taxa identified as cyanobacteria or 'unclassified' to the phylum level were removed. Oscillation of microbiota abundance and period of oscillation were detected by cosinor analysis using the R package DiscoRhythm.[108] Taxa with $p < 0.05$ over a 24-h oscillation period are reported based on Cosinor analysis.

Processing and analysis of bulk RNA-seq data

Concatenated FASTQ files generated from Illumina were used as input to kallisto,[113] a program that pseudo-aligns high-throughput sequencing reads to the *Mus musculus* reference transcriptome (version 38) and quantifies transcript expression. We used 60 bootstrap samples to ensure accurate transcript quantification. Gene isoforms were collapsed to gene symbols using the Bioconductor package tximport (version 3.4). Genes were filtered to counts per million >1 in at least three samples. The filtered gene list was normalized using a trimmed mean of M-values in edgeR.[114] Oscillation of transcript abundance and period of oscillation were detected using Cosinor analysis using the R package DiscoRhythm.[108] Transcripts with $p < 0.05$ over a 24-h oscillation period are reported. Over-representation analysis of Gene Ontology: Biological Process terms to identify enriched molecular pathways/processes in the top enriched and top rhythmic gene lists was performed with clusterProfiler[115] and PantherDB.[116]

Gut metabolic modules

We leveraged Phylogenetic Investigation of Communities by Reconstruction of Unobserved States (PICRUSt2)[117] for functional inference in the form of Kyoto Encyclopedia of Genes and Genomes (KEGG) orthologs[118] to link 16SrNA genomic information with higher-order functional cellular processes. We extracted Gut Metabolic Modules (GMM)[51] using the Gomixer[119] library in R from the microbiota data of female and male Chow and Hf-Lf samples. We then conducted a circadian analysis on GMM to determine whether sex-specific oscillations in microbial community composition reflect changes in predicted microbial functional pathways. These modules represent a set of manually curated references of metabolic pathways reported to occur in the gut microbiome.[51] DiscoRhythm analysis was then applied to these data.

QUANTIFICATION AND STATISTICAL ANALYSIS

Statistical information, including sample size, mean, and statistical significance values, are shown in the text or the figure legends. A variety of statistical analyses were applied, each one specifically appropriate for the data and hypothesis, using GraphPad Prism 9.3.1 or R version 4.1.0 (R Core Team, 2021[107]). For standard metabolic endpoints, analysis of variance (ANOVA) testing with repeated-measures corrections and Bonferroni posthoc tests were used, with significance at an adjusted $p < 0.05$. Processing of RNA-Seq data was conducted using standardized and published protocols. GraphPad Prism and Adobe Illustrator were used for generating figures. No custom script was used to analyze RNA sequencing data.